Article

Multilevel Distributed Linear State Estimation Integrated with Transmission Network Topology Processing

Dulip Madurasinghe * and Ganesh Kumar Venayagamoorthy

Real-Time Power and Intelligent Systems Laboratory, Holcombe Department of Electrical and Computer Engineering, Clemson University, Clemson, SC 29634, USA; gkumar@ieee.org
* Correspondence: dtmadurasinghe@ieee.org

Abstract: State estimation (SE) is an important energy management system application for power system operations. Linear state estimation (LSE) is a variant of SE based on linear relationships between state variables and measurements. LSE estimates system state variables, including bus voltage magnitudes and angles in an electric power transmission network, using a network model derived from the topology processor and measurements. Phasor measurement units (PMUs) enable the implementation of LSE by providing synchronized high-speed measurements. However, as the size of the power system increases, the computational overhead of the state-of-the-art (SOTA) LSE grows exponentially, where the practical implementation of LSE is challenged. This paper presents a distributed linear state estimation (D-LSE) at the substation and area levels using a hierarchical transmission network topology processor (H-TNTP). The proposed substation-level and area-level D-LSE can efficiently and accurately estimate system state variables at the PMU rate, thus enhancing the estimation reliability and efficiency of modern power systems. Network-level LSE has been integrated with H-TNTP based on PMU measurements, thus enhancing the SOTA LSE and providing redundancy to substation-level and area-level D-LSE. The implementations of D-LSE and enhanced LSE have been investigated for two benchmark power systems, a modified two-area four-machine power system and the IEEE 68 bus power system, on a real-time digital simulator. The typical results indicate that the proposed multilevel D-LSE is efficient, resilient, and robust for topology changes, bad data, and noisy measurements compared to the SOTA LSE.

Keywords: distributed architecture; linear state estimation; synchrophasor measurements; topology processor

1. Introduction

Traditional state estimation was introduced to the power system by Fred Schweppe in 1970 in [1–3] to process available imperfect information (noise, bad data, or false data) [4,5] and produces the best possible estimates for the state variables in consideration. However, the traditional static state estimation is inefficient in estimating state variables in modern power systems. The modern bulk power system is increasingly integrated with inverter-based resources such as solar photovoltaic and wind. The electric power system distribution system is becoming more active with the effect of distributed energy sources, microgrid operations, electric vehicle inclusion, spot loads, and demand response programs, which aggregate at substations, thereby influencing the transmission network. Furthermore, the modern world is moving towards an integrated energy system, where other critical energy infrastructures, including natural gas and transportation, are corporately operated with the electrical power system for improved energy efficiency [6], and the modern power system is influenced by factors outside the energy control centers' operation. State estimation is foundational for applications such as security-constrained optimal power flow [7], economic dispatch [8], contingency analysis [9], and security assessment [10]. Thus,

an efficient approach for state estimation is favorable over the traditional state estimation in the modern power system.

State-of-the-art (SOTA) linear state estimation (LSE) has improved the estimation capabilities [11], where efficient measurements are used to establish a linear relationship with the state variables. LSE can accurately estimate bus node voltage phasors utilizing measurements such as available the noisy voltage phasor and current phasor measurements. LSE can be implemented solely based on the phasor measurement units (PMUs) [12] and the network model. The network model of the SOTA LSE is derived from the SOTA transmission network topology processing (TNTP) approach, which is based on the asynchronous supervisory control and data acquisition (SCADA) monitoring of relay signals (SMRS), where the reliability can be challenged [13,14] and only updates the topology from 2 s to 5 s [15]. Furthermore, the SOTA LSE is not scalable for large power systems, because computation time increases rapidly with the size of the network. The power system transmission network is a large, geographically distributed network. Thus, a distributed architecture is favorable to ensure the efficient process of the LSE with PMU measurements.

A comprehensive analysis of the state estimation has been conducted in [16], where shortcomings of the literature and existing operational state estimations have been identified, including accuracy and security. In [17], a robust hybrid state estimator was built against the non-Gaussian noise in PMU measurements; the filtration process utilized SCADA-based state estimation, which still limits the efficiency achieved by the PMU-only state estimation. Distributed state estimation architectures for multiarea power systems have been proposed in [8,18–20]. The different architectures utilize the least squares estimation techniques and information exchange between the control areas. Although distributed architecture improves computational efficiency, the approaches are based on traditional iterative estimation methods, where the efficiency is compromised. A semidefinite programming formulation based on distributed state estimation utilizing synchrophasor measurements was studied in [21]. Both proposed approaches in [21] involve the legacy SE and the PMU-based linear estimation, which increase the computational burden. The incorporation of linear and nonlinear models for state estimation has been investigated in [22]. The system is divided into multiple linear and nonlinear areas, which define the distributed architecture of the study. The procedure is expected to be completed based on sequential flow, where the efficiency achieved from PMU measurement-based LSE in the linear regions is compromised. PMU-based topology derivation and extended LSE implementation were studied in [23], where the test system used the breaker status as a digital input to the PMU. Digital inputs in the PMUs require additional communication network upgrades from relays or remote terminal units (RTUs) to PMUs in the substation; furthermore, the proposed approach is centralized. A phasor data-based state estimator with phase bias correction has been proposed in [24]. This work identifies PMU-available high-voltage substations for building phasor state estimators. Identifying the island topology is critical; although, using SMRS in this study limits the efficiency of the overall procedure. A two-level LSE has been proposed in [25–27]; the proposal investigates the power system at the substation level and network level. The shortcomings of this approach are that the only redundancy for the substation level is the network level, where the computational overhead is high in larger networks. Furthermore, the study was limited to the ring bus arrangement type (RBA) substations only. The effectiveness of the overall approach can be different based on the type of substation arrangement.

A physics-based hierarchical TNTP (H-TNTP) approach based solely on node voltages and branch currents measurements utilizing artificial intelligence algorithms was proposed in [28]. H-TNTP can be used to derive the substation area network-level topologies using current and voltage measurements, which is ideal for a distributed LSE architecture. An efficient H-TNTP can be established by incorporating the synchrophasor network (H-TNTP-PMU), which updates the transmission network topology at every PMU frame. The synchrophasor network typically delivers voltage and current phasor measurements at 30 Hz [29]. Thus, incorporating H-TNTP-PMU will enable LSE execution at every PMU

measurement. This paper proposes a multilevel distributed LSE (D-LSE) architecture with substation-level and area-level estimation utilizing H-TNTP-PMU. The network level based on the SOTA LSE enhanced with the H-TNTP-PMU has been integrated as the redundancy level for the area level. The proposed approach overcomes the limitations identified in the SOTA LSE and the alternative approaches proposed by other researchers. The D-LSE incorporates the efficient and reliable H-TNTP-PMU as the topology processor, which enables the completion of the overall procedure at the PMU rate. The multilevel redundancy improves the reliability of the D-LSE. Incorporating all typical substation arrangements in the substation level ensures the applicability of the proposed D-LSE. The overview of the proposed D-LSE is shown in Figure 1.
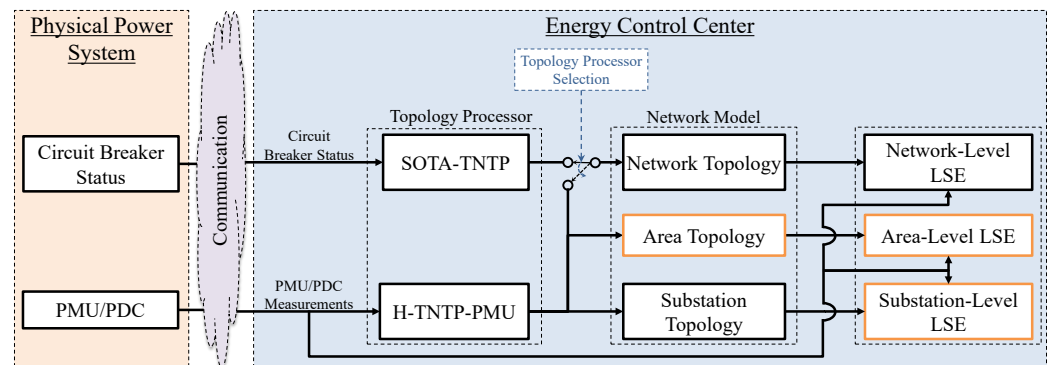
Figure 1. Distributed linear state estimation (D-LSE) integrated with the state-of-the-art (SOTA) linear state estimation (LSE). The 'orange-line' blocks present the contribution of this work.

The main contributions of this paper are the following:

- A multilevel distributed linear state estimation has been developed based on hierarchical transmission network topology processing. With the developed D-LSE, substation bus voltage phasors can be estimated at the substation level and/or area level. This caters to fast and efficient linear state estimation for large power systems.
- The traditional linear state estimation has been enhanced with H-TNTP-PMU to provide a network-level model that is updated with the same measurements used for LSE. This improves the accuracy of the traditional LSE.
- The D-LSE and enhancement to the traditional LSE have been illustrated on two benchmark test power systems. The two power systems, one small and the other medium, have been implemented on a real-time power system simulator with phasor measurement units and noisy measurements. The typical results obtained with the D-LSE and enhanced LSE demonstrate better efficiency, resilience, and robustness with respect to topology changes, bad data, and noisy measurements, respectively.

The rest of the paper is organized as follows: Section 2 presents the formulation of the proposed D-LSE architecture with the enhanced network-level estimation. An introduction to the test power system models, typical results, and the performance analysis for D-LSE with the enhanced network-level estimation are discussed in Section 3. The conclusion and future directions are provided in Section 4.

2. Methodology

The methodology section outlines the LSE formulation for the proposed D-LSE with the enhanced network-level estimation, thus providing a comprehensive clarification of its components and organization.

2.1. Linear State Estimation (LSE)

The SOTA LSE considers the entire power system to be a single entity. The formulation of the LSE described in [11] is considered for the network level as a redundancy layer for the D-LSE and to compare with substation-level and area-level estimation. The current

measurement bus incidence matrix (A) presents the current flow measurement's location in the network, where the TNTP is used to update. A is an m by b-sized matrix, where m represents the number of current measurements in the network, and b is the number of buses that have current measurements leaving the selected bus. The voltage measurement bus incidence matrix (II) is similar to the A, where the TNTP is used to update. It presents the relationship between a voltage measurement and its respective location in the network. It is an n by d matrix, where n represents the number of voltage measurements in the network, and d is the number of buses with voltage measurements. The series admittance matrix (y) is a diagonal matrix, where the diagonal elements are the measured admittance of the respective lines. It is k by k-sized matrix, where k represents the number of branch current measurements in the network. The shunt admittance matrix (y_s) relates the location of each current measurement to the shunt admittance of the line it measures. It is an l by g matrix, where l is the number of current measurements in the network, and g is the number of buses where the current is being originally measured. The intermediate characteristics matrix $[B]$ can be formed with A, II, y, and y_s using (1).

$$[B] = \begin{bmatrix} II \\ yA + y_s \end{bmatrix} \tag{1}$$

The linear relationship between measurements and the states can be formulated using (2). $[r]$ is referred to as the measurement residue vector.

$$[z] = [B][x] + [r] \tag{2}$$

Considering that the measurements contain noise, the covariance matrix (W) appears in the solution. Then, the solution can be found using (3).

$$[x] = \left[\left(B^T W^{-1} B \right)^{-1} B^T W^{-1} \right][z] = [H][z] \tag{3}$$

2.2. Multilevel Distributed Linear State Estimation (D-LSE)

LSE at every PMU rate can be computationally challenging when considering the enormity of power systems. A preliminary experiment has been conducted to understand the computation overhead of the LSE procedure with respect to the network size. The computation overhead is shown in Figure 2.
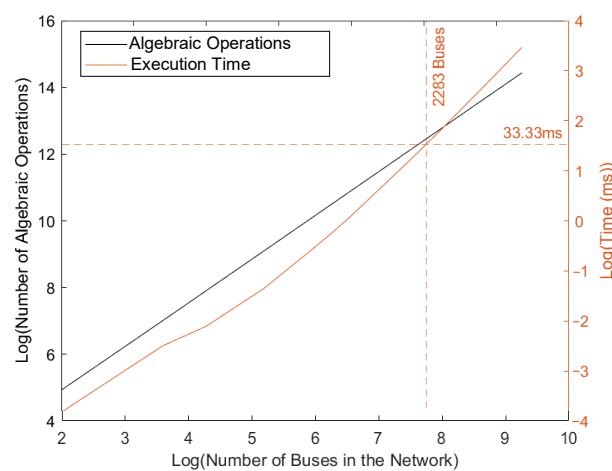
Figure 2. Log-scaled number of algebraic operations and execution time for LSE procedures (excluding H-TNTP computation).

Considering the overall LSE procedure discussed in Section 2.1, the number of algebraic operations and execution time are estimated for different bus-sized networks. The

execution time is the computation time for matrix formation and the solution to the LSE equation in (3). The execution time is estimated by running the LSE algorithm in a dedicated node of the Clemson University Palmetto Cluster with 124 GB of memory. The computation overhead exponentially increased with the number of buses in the considered network, as shown in Figure 2. Based on the highest execution time (on the computation platform mentioned above) for executing the LSE under the PMU data rate (under 33.33 ms), the network size limit came out to 2283 buses, excluding the computation time for TNTP and communication delays. Thus, SOTA LSE is not an option for practical implementation in large power systems. Though the efficiency limitation of the SOTA LSE approach has been identified, SOTA LSE (network level) is considered a redundancy level to the area level. Furthermore, the network level will be used to compare performance with the D-LSE. The flow diagram of the procedure of the D-LSE with the enhanced network level is shown in Figure 3.
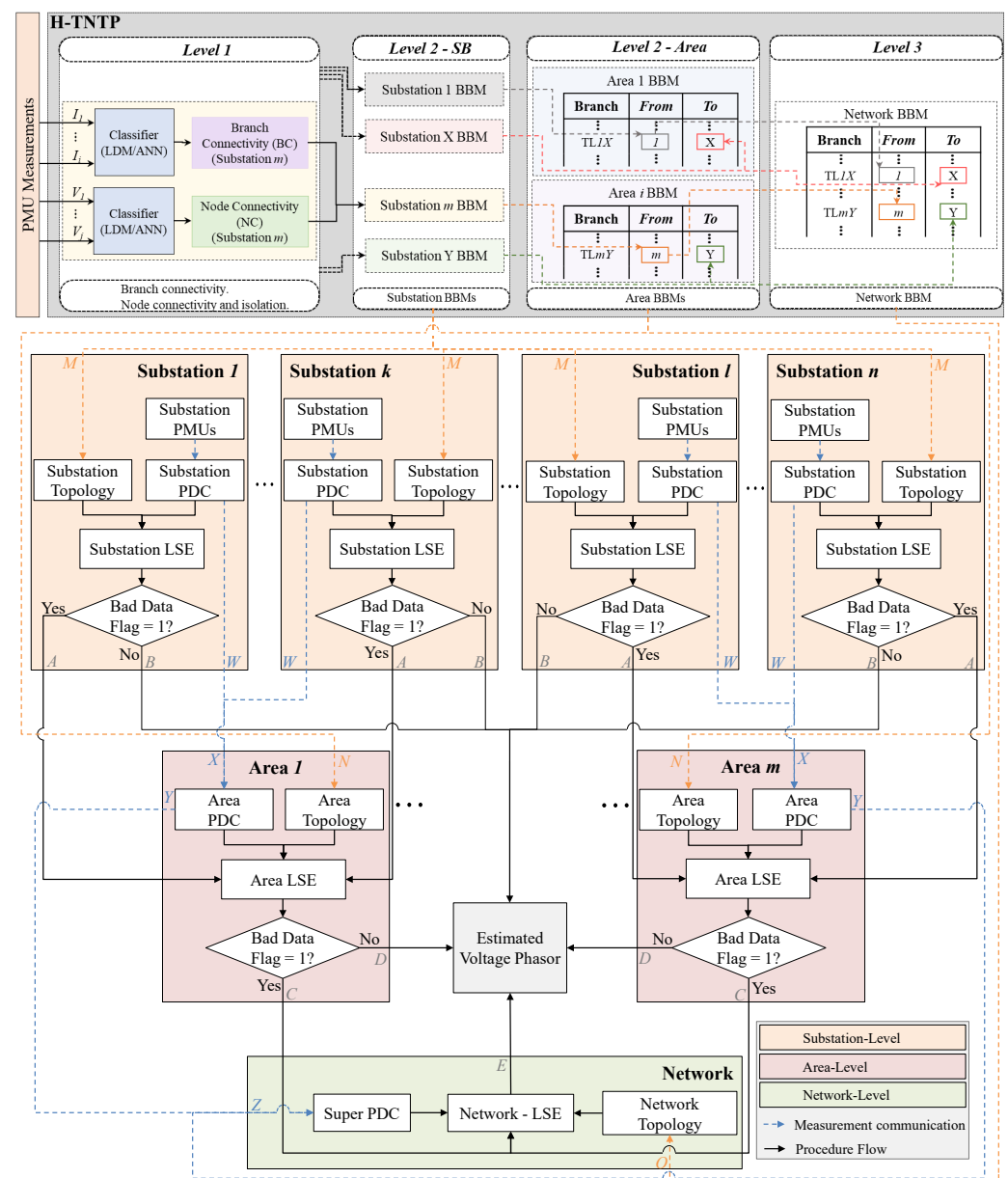
Figure 3. Flow diagram of the proposed distributed LSE (D-LSE), including network level integrated with hierarchical transmission network topology processing based on synchrophasor measurements (H-TNTP-PMU) [28].

Based on the above preliminary study, it was identified that a more computationally efficient architecture for LSE is required for large multiarea power systems. Hence, the authors proposed the D-LSE architecture. The H-TNTP approach was modified to accommodate the D-LSE, as shown in Figure 3, including the area level BBM as Level 2-Area. Thus, the area level of the D-LSE will be based on Level 2-Area of the modified H-TNTP. Similarly, for the substation level of the D-LSE, H-TNTP Level 2-SB was utilized as the topology, and for the network level, Level 3 of the H-TNTP was used. The LSE can then be performed for each area and substation by keeping all PMU measurements relative to the global reference (ground in practical use). This allows substation-level or area-level D-LSE to be implemented in parallel processes.

2.3. Substation Level

A substation consists of branches, bus sections, protection equipment (relays), measurement instruments (PMUs), and switching equipment (breakers, isolators, etc.). Each piece of equipment is required for the power system's operation and control. H-TNTP Level 2-SB shown in Figure 3 can be directly utilized to identify the substation topology. Substations are considered to be zero-impedance networks. Since Ohm's law-based current, voltage, and impedance relationships cannot be established on a zero-impedance network, a linear relationship for currents based on the substation configuration was established following the method proposed in [25]. This is shown in Figure 3 at the substation level and elaborated in Figure 4a.
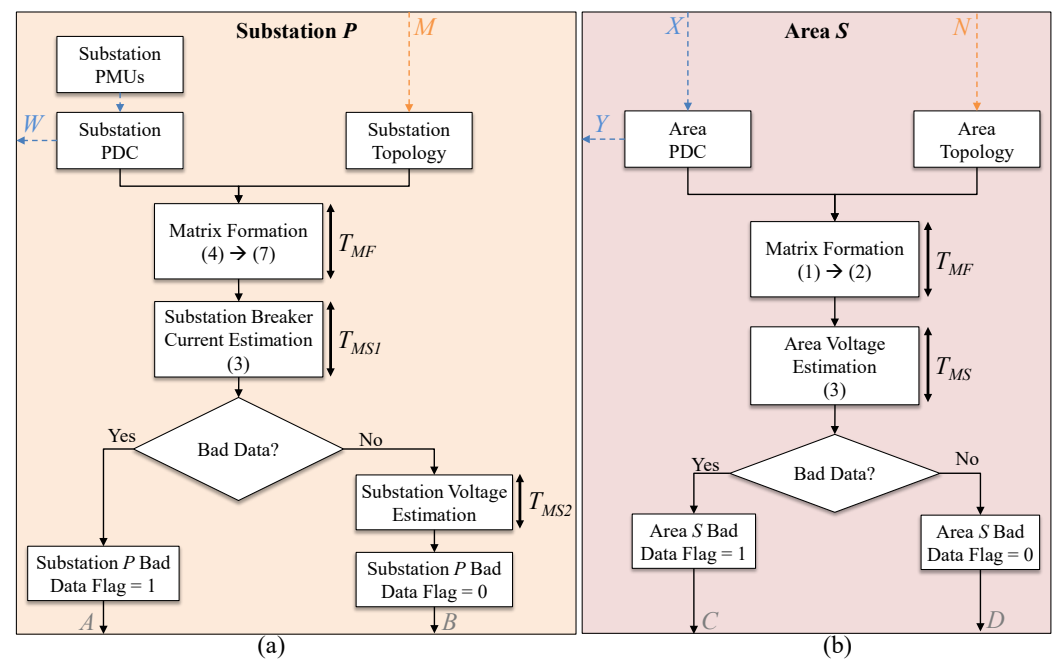
Figure 4. (**a**) Flow diagram of the proposed D-LSE at the substation level considering Substation P as an example. LSE procedure flow paths A and B, measurement communication path W, and H-TNTP-PMU topology path M are referred to in Figure 3. (**b**) Flow diagram of the proposed D-LSE at the area level considering Area S as an example. LSE procedure flow paths C and D, measurement communication paths X and Y, and H-TNTP-PMU topology path N referred to in Figure 3.

The proposed substation level LSE comprises two estimations: current state estimation and voltage state estimation. The current estimation is used for bad data detection in analog current measurements and topology errors; voltage-based bad data identification can be implemented using cellular computational networks (CCNs) [30]. When the bad data are detected at the substation level, the substation LSE raises a flag and entrusts the LSE to the area level. This is based on the assumption that bad data detection indicates a faulty PMU. Thus, the voltage phasor can also be a bad measurement. Thus, this avoids conducting

simple weighted average estimation for the voltage phasor, which does not have inherent bad data detection. The T_{MF} is the computational time for matrix formation, T_{MS1} is the computational time to solve breaker current estimation, and T_{MS2} is the computational time to solve voltage estimation using a weighted average. The area-level LSE will use the bad data detection flag and conduct the area-level LSE, thereby avoiding bad data flagged substations in the area.

The current state estimation considers the circuit breaker currents as states in the LSE. Based on Kirchhoff's Current Law (KCL), the relationship between the circuit breaker current and the injection currents in the zero impedance network can be written as (4). z_{inj} refers to the current injection by each node, and $A_{breaker}$ is the adjacent matrix that defines the relationship, which is the node connectivity matrix (NCM) of the H-TNTP Level 2. r_{inj} is the injection current measurement residue.

$$[z_{inj}] = [A_{breaker}][x] + [r_{inj}] \tag{4}$$

Based on the availability of the breaker current measurement, another linear relationship can be established for the breaker currents by relating the breaker current estimation to the measurements with an identity matrix, as shown in (5). $z_{breaker}$ refers to the breaker current measurements, I is the identity matrix, and $r_{breaker}$ is the breaker current measurement residue.

$$[z_{breaker}] = [I][x] + [r_{breaker}] \tag{5}$$

By combining (4) and (5), a single linear state estimation problem can be formed as (6), which again can be summarized in the form shown in (2), where the B matrix given in (7) consists of 1, 0, and -1 as elements.

$$[z] = \begin{bmatrix} z_{inj} \\ z_{breaker} \end{bmatrix} = \begin{bmatrix} A_{breaker} \\ I \end{bmatrix} x + \begin{bmatrix} r_{inj} \\ r_{breaker} \end{bmatrix} \tag{6}$$

$$[B] = \begin{bmatrix} A_{breaker} \\ I \end{bmatrix} \tag{7}$$

Voltage state estimation is conducted at the substation level if no bad data are detected. The voltage state estimation is an equal-weighted average estimation considering all available voltage measurements at the substation. If the substation is split (in the case of ring bus arrangement (RBA), main and transfer bus arrangement (MTBA), double bus single breaker arrangement (DBSBA), double bus double breaker arrangement (DBDBA), or breaker and half arrangement (BHA) [31]), the weighted average will be performed for the two separated sections of the substation by individually utilizing respective node voltage measurements.

The traditional normalized residual test using (8) is considered in this study for bad data detection for the D-LSE approach. The state vector estimation is $\hat{x}$, z_i is measurement i, and $h_i(\hat{x})$ is the measurement i as a function of the estimated state vector; Ω is calculated using (9).

$$NR(i) = \frac{|(z_i - h_i(\hat{x}))|}{\sqrt{\Omega_{i,i}}} \tag{8}$$

$$\Omega = W - B(B^T W^{-1} B)^{-1} B^T \tag{9}$$

2.4. Area Level

The area level of the D-LSE will be utilized only if bad data detection is flagged in the substation level of the D-LSE. It is important to note that substation-level bad data detection is flagged only for breaker current measurements. Thus, there is a possibility that bad voltage measurement data can be available at the area level. The area level of the proposed D-LSE is shown in Figure 4b.

Figure 3 shows how the area level is fitted in the D-LSE. The T_{MF} is the computational time for matrix formation, and T_{MS} is the computational time for voltage estimation. When there is bad data detection at the substation level, a bad data detection flag is sent to the area level. The area level will be based on the LSE formulation explained under Section 2.1. LSE will be formulated by intentionally neglecting bad measurements in the detected substation, thus improving the estimation accuracy. The area's topology can be derived from the substation BBMs in the considered area, as shown in Figure 3 for the Level 2-Area in the H-TNTP.

2.5. Network Level

The network level will be utilized only if more bad measurements are flagged in the area level of the D-LSE after bypassing the substation level due to bad current measurements being detected. The enhanced network level integrated as the redundancy level for the area level of the D-LSE is shown in Figure 3 and elaborated in Figure 5. The T_{MF} is the computational time for matrix formation, and T_{MS} is the computational time for voltage estimation. Under bad data detection at the area level, a bad data flag is sent to the network level with the identified bad voltage measurements of the area. The network level will be based on the SOTA LSE formulation explained under Section 2.1. LSE will be formulated by intentionally neglecting the bad measurements detected, thus improving the estimation accuracy at the network level. The network topology can be retrieved from the H-TNTP Level 3 as shown in Figure 3.
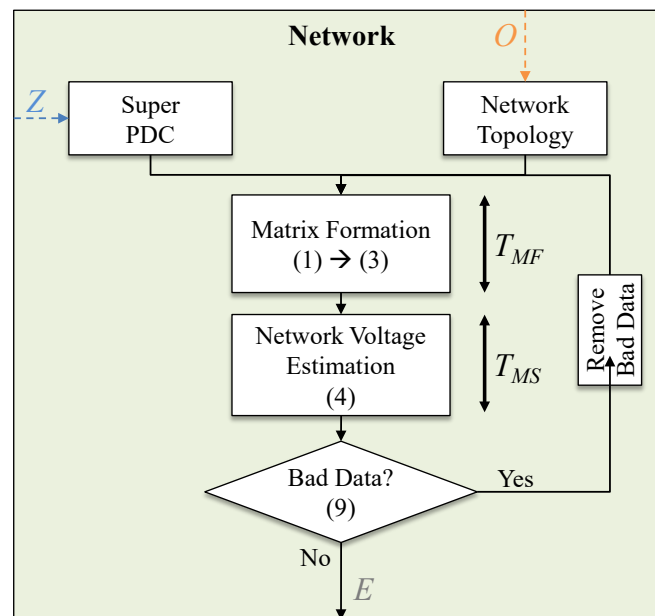
Figure 5. Flow diagram of the network level. LSE procedure flow path E, measurement communication path Z, and H-TNTP-PMU topology path O are referred to in Figure 3.

3. Results and Discussion

This study considered two power system models, the modified two-area four-machine power system and the IEEE 68 bus power system, for implementing the D-LSE. All three level results are presented under topology changes and with bad data in the measurements for the modified two-area four-machine power system. For the IEEE 68 bus power system, the area-level and network-level results are presented. In the results tables, magnitude quantities are in per unit (pu) and indicated by "M (pu)". Angle quantities are in degrees and indicated by "∠ °". It is important to note that all the test results presented except for Sections 3.1.1 and 3.2.1 have considered the fully connected topology of the networks.

The PMUs implemented in the RTDS simulation provided noise-free measurements, which are defined as the *True Value*. The PMU measurement errors were regulated by the

total vector error (TVE), which is the difference between the true phasor and the measured phasor. The standard maximum permissibility of the TVE is 1% [32]. To mimic the reality of the PMU measurements, a Gaussian white noise (GWN) was added to all *True Values* at the simulator, thus defined as the *Measurement*. The GWN is a zero mean, user-defined level of variance noise addition to the signal using (10). To analyze the performance of the D-LSE, 5% of the noise level (variance) was considered in all experiments.

$$Measurement = True\ Value + n;\ where\ n \sim N(0, \sigma^2) \tag{10}$$

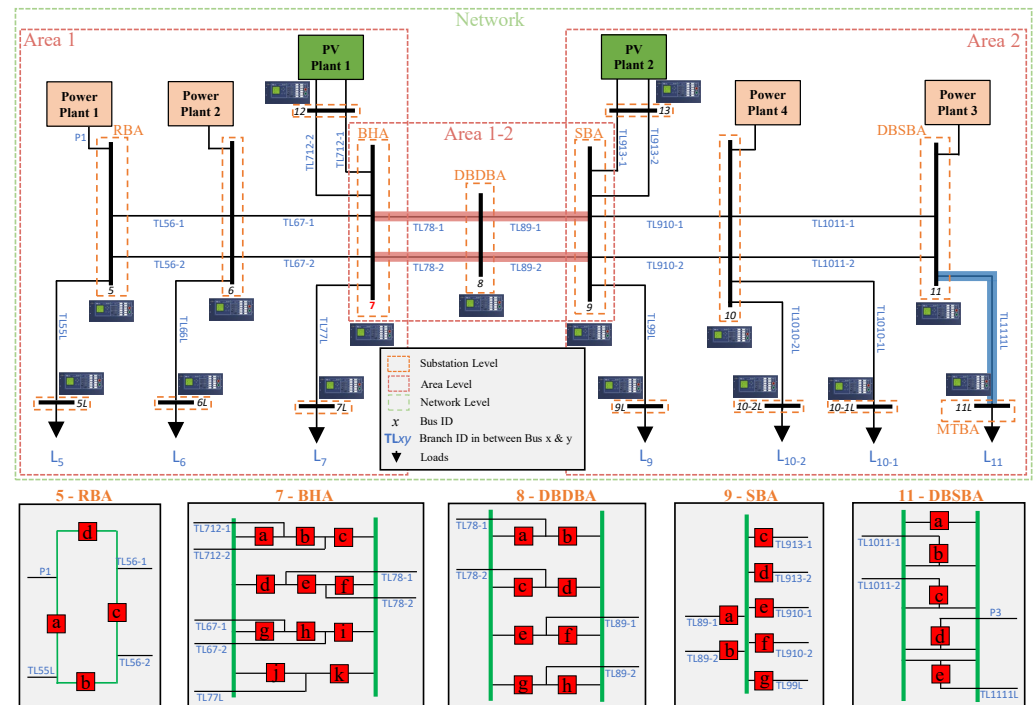### 3.1. Modified Two-Area Four-Machine Power System (System 1)

The benchmark two-area symmetric system consists of five buses and two machines in each area, thus representing each substation with a single bus. Two double-circuit tie lines connect the two areas through a tie-line bus. As shown in Figure 6, the modified two-area four-machine power system model consists of four conventional synchronous generator-based power plants and two additional solar power plants. The modified system contains seven loads at bus 5L, 6L, 7L, 9L, 10-1L, 10-2L, and 11L. The modified two-area four-machine power system model with all typically used substation arrangements has been considered [28]. All conventional generators were configured with turbine governors, automatic voltage regulators, and power system stabilizers. The simulation used the RSCAD FX 2.1 software on the Real-Time Digital Simulator (RTDS) [33]. RSCAD software PMUs were utilized as the measurement instruments for this study. Substation 9 was configured as a single bus arrangement (SBA). The SBA was the fundamental arrangement. The reliability of the SBA is low due to a lack of redundancy under breaker, isolator failure, or bus fault. Due to the lack of reliability, using the SBA is limited in practice. Substation 11L was configured as an MTBA. It is important to highlight that the MTBA acts as an SBA substation under normal operation (transfer bus on standby). Thus, the MTBA was not considered in the test cases. Substation 5 was configured as an RBA. Substation 11 was configured as a DBSBA. Substation 8 was configured as a DBDBA. Substation 7 was configured as a BHA. All other substations were configured as SBAs. Further information on each substation arrangement type can be found in [28]. PMUs were installed in each substation. Thus, the current phasor measurements of each branch connecting to any substation, node voltages, and breaker currents are available. The H-TNTP-PMU was implemented based on the node voltage and branch current phasor measurements from the PMUs. PMUs were collecting measurements at 30 Hz. Three areas were identified for the D-LSE area level in the modified two-area four-machine system, as shown in Figure 6. The selection was made since Substation 8 was not included in either Area 1 or Area 2. Thus, an additional area was designated to cover Substations 7, 8, and 9 as Area 1–2. Thus, D-LSE Area 1 included the 5G, 5, 5L, 6G, 6, 6L, 12, 7, and 7L substations. Area 1–2 included Substations 7, 8, and 9. Area 2 encompassed Substations 9, 13, 9L, 10G, 10, 10-1L, 10-2L, 11G, 11, and 11L.

The estimation's accuracy assessment was based on error reduction. An error reduction factor (*ERF*), calculated in (11), indicates the estimation accuracy as many-fold better than the measurement (noisy or bad) received. The *ERF* is calculated by taking the inverse of the ratio of the absolute deviation between the estimated state and *True Value* against the *Measurement* and *True Value*. The *ERF* is a unitless metric.

$$ERF_i = \frac{|Measurement_i - True\ Value_i|}{|Estimated_i - True\ Value_i|} \tag{11}$$

For accuracy, each test case voltage estimation was analyzed based on the *ERF*. It is important to emphasize that the *ERF* for the voltage estimation in SBA type was neglected, since the SBA only considers the available single bus voltage measurement as the estimated value from the weighted average. Furthermore, the SBA is an unreliable arrangement with limited practical use in the transmission network.

Table A1 presents the voltage estimates for all the substations under all three levels when independently operated. Furthermore, the *ERF* for the voltage estimation of all three levels is shown in Table A1. Based on these results, the overall best accuracy under GWN was determined at the substation level.

Figure 6. Modified two-area four-machine power system model indicating substation level, area level, and network level. Topology was changed from Topology S1A (fully connected network) to Topology S1B by removing TL1111L (single line outage), which is indicated in blue. Topology was changed from Topology S1A to Topology S1C by removing two double circuit tie lines, TL78-1, TL78-2, TL89-1, and TL89-2 (area separation), which is shown in red. Breakers in each substation are identified with lowercase letters.

3.1.1. Steady State with Gaussian White Noise for Topology Change

The D-LSE was tested for the topology changes detected by H-TNTP-PMU [28]. The topology changes from Topology S1A (fully connected network) considered for the modified two-area four-machine power system are Topology S1B and Topology S1C. The topology changes were selected in accordance with the test cases presented in [28], which elaborates the topology processing with H-TNTP-PMU. The topology was changed from Topology S1A to Topology S1B by removing TL1111L (single line outage). In the next experiment, the topology was changed from Topology S1A to Topology S1C by removing the double circuit tie lines, TL78-1, TL78-2, TL89-1, and TL89-2 (area separation), as shown in Figure 6. The H-TNTP-PMU outputs are shown in Figure 7. The pretopology change (from Topology S1A to Topology S1B or Topology S1C) matrix values are shown in orange, and the post-topology change values are shown in black. Table A1 presents the steady state voltage estimation for all three levels of the D-LSE in Topology S1A. Table 1 presents the steady state voltage estimation for all three levels in Topology S1B and Topology S1C. Due to the change in topology from Topology S1A to Topology S1B, Substation 11L was isolated. Due to the change in topology from Topology S1A to Topology S1C, Substation 8 was isolated. The performance of the three levels was tested during the transition from Topology S1A to Topology S1B and Topology S1A to Topology S1C. Furthermore, both topology transitions were conducted under SOTA TNTP, which typically updates the topology in 2 s to 5 s [15] and H-TNTP-PMU, which typically updates the topology in every PMU data frame [28]. The topology change experiment followed the setup shown in

Figure 8. The substation-level, area-level, and network-level estimations for Substation 11, which were directly affected by Topology S1A to Topology S1B (TL1111L single line outage) transition, are shown in Figures 9 and 10 under both H-TNTP-PMU and SOTA TNTP. The substation-level and area-level estimations for Substation 7, which were directly affected by Topology S1A to Topology S1C (area separation) transition, are shown in Figure 11 under both H-TNTP-PMU and SOTA TNTP. The start of the transition is indicated using "P", and the SOTA TNTP detection of the topology change is indicated using "Q" in the Figures 9–11. It can be seen that H-TNTP-PMU-based D-LSE and enhanced network-level LSE had an accurate estimation compared to the inefficient SOTA TNTP-based D-LSE and enhanced network-level LSE.

Substation 11L (NCM)

Node	1
1	1 ¦ 0

Substation 11 (NCM)

Node	1	2	3	4	5	6
1	1¦1	1¦1	1¦1	1¦1	1¦1	1¦1
2	1¦1	1¦1	1¦1	1¦1	1¦1	1¦1
3	1¦1	1¦1	1¦1	1¦1	1¦1	1¦1
4	1¦1	1¦1	1¦1	1¦1	1¦1	1¦1
5	1¦1	1¦1	1¦1	1¦1	1¦1	1¦1
6	1¦1	1¦1	1¦1	1¦1	1¦1	1¦1

Area 2

Branch	Status
TL89-1	1 ¦ 1
⋮	⋮ ¦ ⋮
TL1010-2L	1 ¦ 0
L10-1L	1 ¦ 0
⋮	⋮ ¦ ⋮
TL1111L	1 ¦ 1

Network

Branch	Status
TL55L	1 ¦ 1
⋮	⋮ ¦ ⋮
TL1010-2L	1 ¦ 0
L10-1L	1 ¦ 0
⋮	⋮ ¦ ⋮
TL1111L	1 ¦ 1

(a)

Substation 7 (NCM)

Node	1	5	6
1	1¦1	1¦0	1¦0
5	1¦0	1¦0	1¦0
6	1¦0	1¦0	1¦0

Substation 8 (NCM)

Node	1	6
1	1¦0	1¦0
6	1¦0	1¦0

Substation 9 (NCM)

Node	1
1	1¦1

Area 1

Branch	Status
TL55L	1¦1
⋮	⋮¦⋮
TL78-1	1¦0
TL78-2	1¦0

Area 1-2

Branch	Status
TL127-1-1	1¦1
⋮	⋮¦⋮
TL78-1	1¦0
TL78-2	1¦0
TL89-1	1¦0
TL89-2	1¦0
⋮	⋮¦⋮
TL99L	1¦1

Area 2

Branch	Status
TL89-1	1¦0
TL89-2	1¦0
TL1010-2L	1¦1
L10-1L	1¦1
⋮	⋮¦⋮
TL1111L	1¦1

Network

Branch	Status
TL55L	1¦1
⋮	⋮¦⋮
TL78-1	1¦0
TL78-2	1¦0
TL89-1	1¦0
TL89-2	1¦0
⋮	⋮¦⋮
TL1111L	1¦1

(b)

Figure 7. The topology change detected by H-TNTP-PMU Level 2-SB, Level 2-Area, and Level 3 [28]. (**a**) Topology S1A (fully connected) to Topology S1B. (**b**) Topology S1A to Topology S1C.
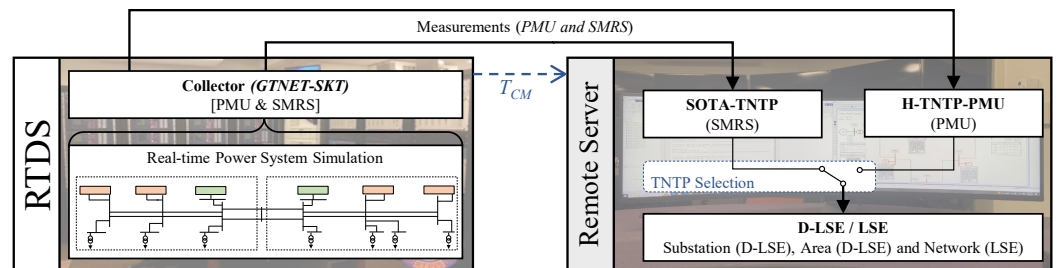
Figure 8. Experiment setup for executing D-LSE for H-TNTP-PMU and SOTA TNTP.

3.1.2. Steady State with Gaussian White Noise and Circuit Breaker Current Bad Data

The substation level of the D-LSE was tested for bad data. The bad data considered in the experiment were based on a common human error: connecting wires in reverse polarity. Thus, the bad data will be the reverse phasor of the *Measurement* received. At the substation, a circuit breaker current of bad data was applied. The current estimations of the substation level of the D-LSE for the BHA substation arrangement are presented in Table 2. The measurements highlighted in red are the bad data. The measurements highlighted in blue are the noisy measurements directly affected by the bad data. The normalized residual was used to detect and identify the bad data in the measurements. As it can be seen in Table 2, a single circuit breaker current bad data can negatively influence the related noisy measurements, which is the basis for handing over the voltage estimation to the subsequent level.
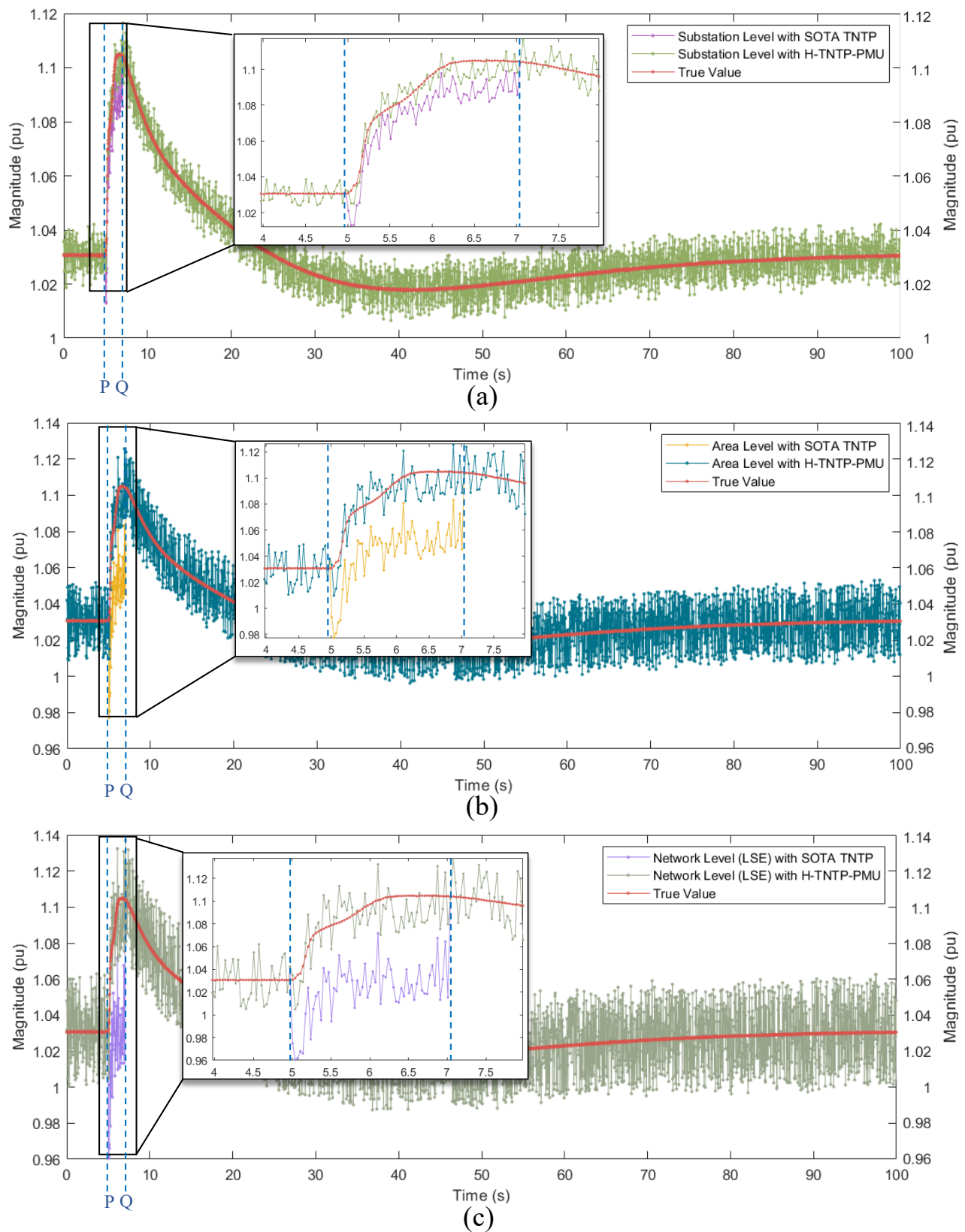
Figure 9. Voltage phasor magnitude estimation of the Substation 11 during the Topology S1A to Topology S1B change. (**a**) Substation level. (**b**) Area level. (**c**) Network level.
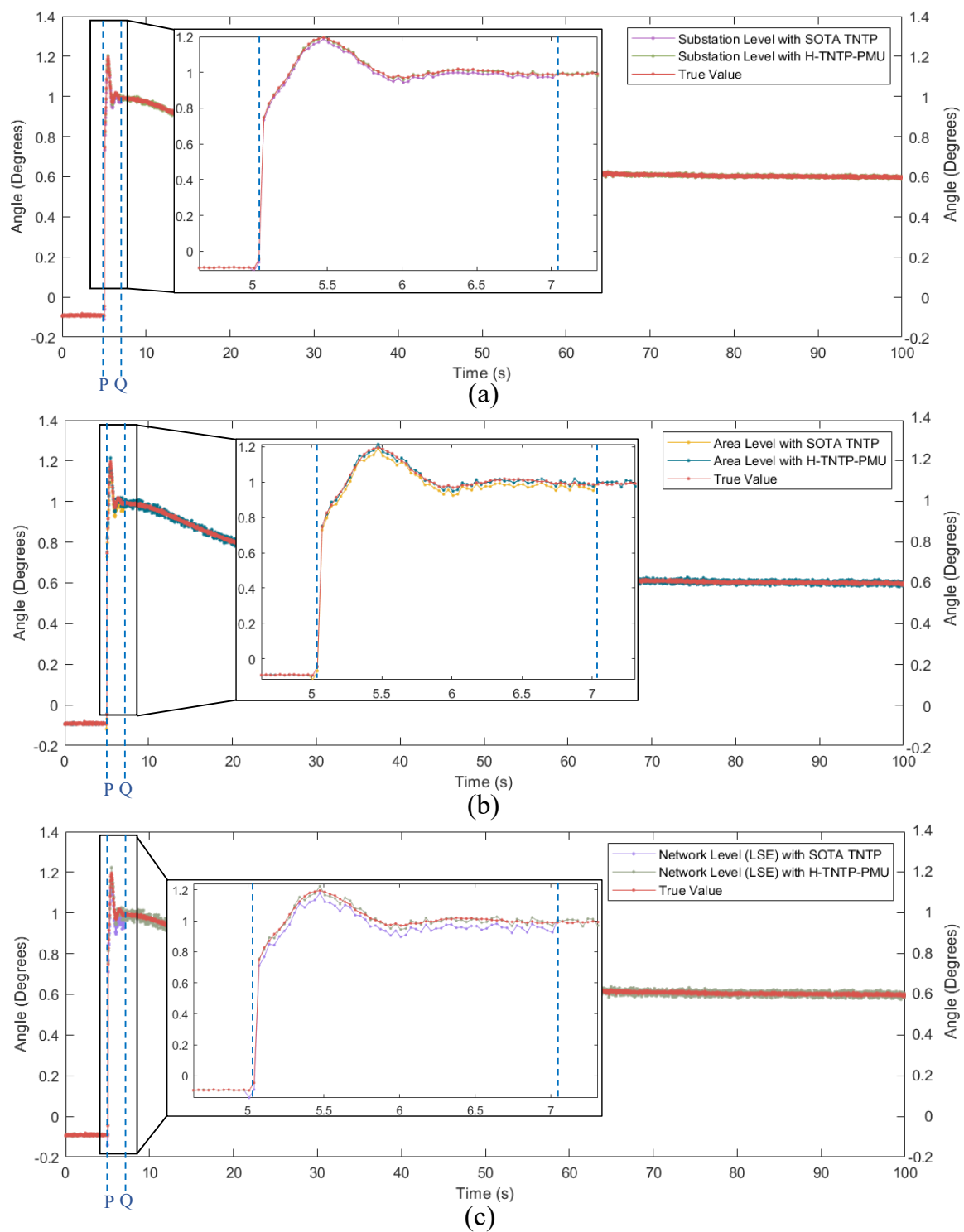
Figure 10. Voltage phasor angle estimation of the Substation 11 during the Topology S1A to Topology S1B change. (**a**) Substation level. (**b**) Area level. (**c**) Network level.
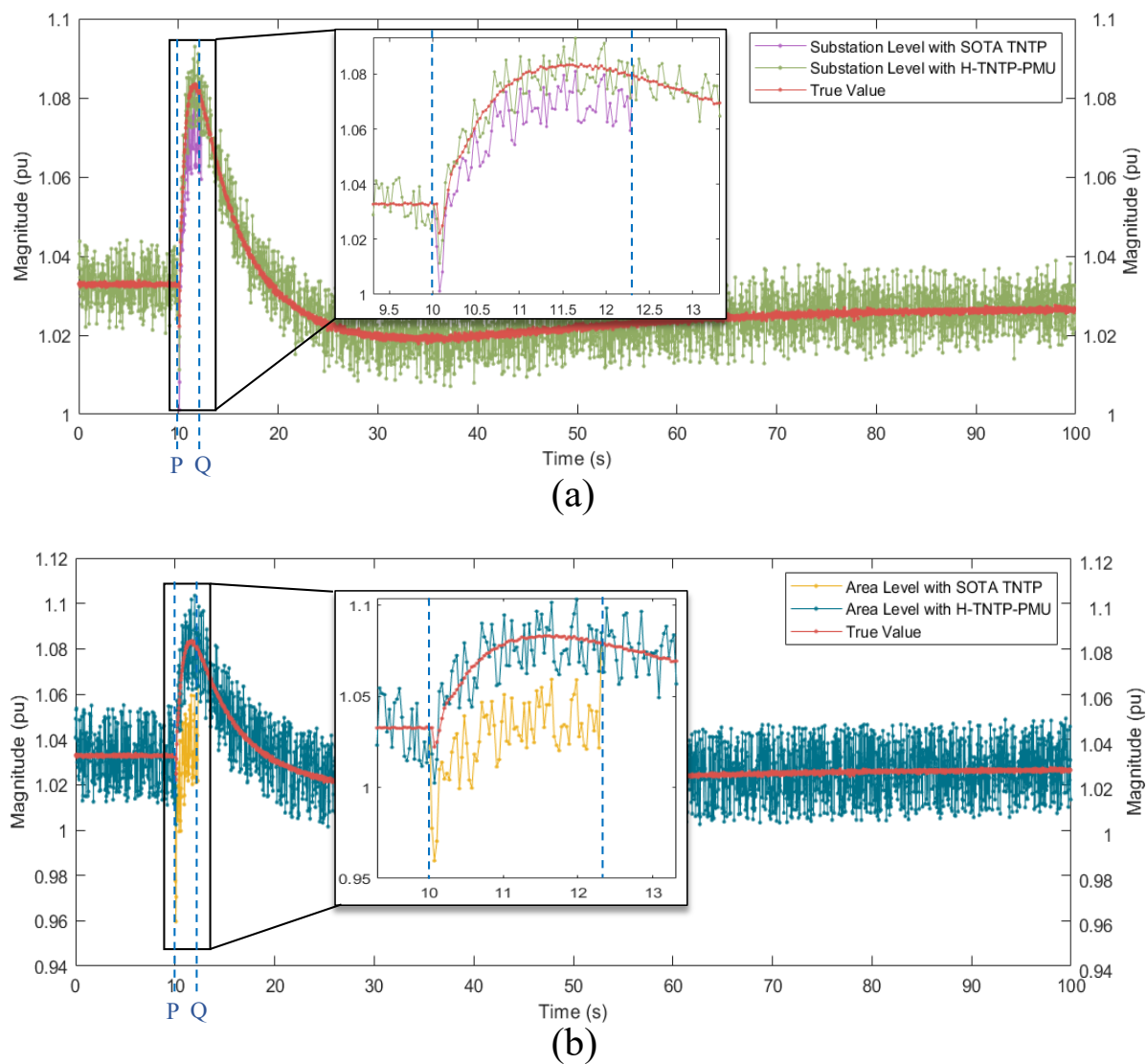
Figure 11. Voltage estimation of Substation 7 during the Topology S1A to Topology S1C change. (**a**) Substation level. (**b**) Area level.

3.1.3. Steady State with Gaussian White Noise, Circuit Breaker Current Bad Data, and Injection Current Bad Data

The substation level of the D-LSE was tested for the inclusion of multiple bad data. A circuit breaker current with bad data and a single injection current with bad data were included at the substation. The current estimation of the substation level of the D-LSE for the BHA substation arrangement is presented in Table 3. As seen in Table 3, a single circuit breaker current and a single injection current with bad data significantly influenced the other related measurements and the substation-level estimation accuracy. Although the estimation was more accurate in the substation level under noisy conditions, as shown in the Table A1 results, the bad data highly deviated from the accuracy of the substation-level estimation. Thus, the state estimation was handed over to the area level under bad data detection at the substation level.

Table 1. Voltage estimation from the substation level, area level, and network level for modified two-area four-machine power system model under a steady state for Topology S1B (single line outage) and Topology S1C (area separation). Magnitude ("M") is shown in pu, and the angle (∠) is in degrees (°).

ID	Topology S1B										Topology S1C									
	Measurement		*True Value*		Substation Level		Area Level		Network Level		*Measurement*		*True Value*		Substation Level		Area Level		Network Level	
	M (pu)	∠°	M (pu)	∠°	M (pu)	∠°	M (pu)	∠°	M (pu)	∠°	M (pu)	∠°	M (pu)	∠°	M (pu)	∠°	M (pu)	∠°	M (pu)	∠°
5	1.058	34.723	1.031	34.608	1.036	34.630	1.041	34.652	1.046	34.678	1.024	−17.281	1.027	−17.359	1.027	−17.340	1.026	−17.331	1.025	−17.317
5L	1.013	30.516	1.026	30.494	1.013	30.516	1.020	30.504	1.019	30.508	0.973	−13.188	1.022	−13.214	0.973	−13.188	1.002	−13.203	0.991	−13.199
6	1.072	35.226	1.029	35.107	1.072	35.226	1.047	35.155	1.056	35.182	1.051	−18.360	1.024	−18.283	1.051	−18.360	1.036	−18.317	1.038	−18.327
6L	1.034	32.234	1.026	32.361	1.034	32.234	1.029	32.312	1.030	32.289	0.997	−15.488	1.021	−15.506	0.997	−15.488	1.011	−15.499	1.007	−15.496
12	1.063	35.144	1.034	35.161	1.063	35.144	1.046	35.154	1.049	35.152	1.059	−18.658	1.027	−18.614	1.059	−18.658	1.041	−18.630	1.047	−18.637
7	0.999	34.717	1.033	34.784	1.027	34.769	1.020	34.760	1.014	34.746	1.001	−18.318	1.026	−18.240	1.022	−18.249	1.017	−18.270	1.011	−18.288
7L	1.029	33.909	1.031	33.972	1.029	33.909	1.030	33.946	1.030	33.939	0.999	−17.434	1.024	−17.415	0.999	−17.434	1.013	−17.423	1.010	−17.426
8	1.012	31.734	1.041	31.758	1.036	31.755	1.029	31.749	1.023	31.743	-	-	-	-	-	-	-	-	-	-
13	1.002	29.097	1.032	29.241	1.002	29.097	1.020	29.188	1.017	29.157	1.051	27.920	1.033	27.845	1.051	27.920	1.040	27.875	1.043	27.883
9	1.006	28.931	1.031	28.870	1.006	28.931	1.020	28.892	1.015	28.902	1.053	27.391	1.031	27.471	1.053	27.391	1.040	27.442	1.044	27.424
9L	1.067	27.753	1.028	27.785	1.067	27.753	1.044	27.773	1.049	27.765	1.022	26.307	1.029	26.389	1.022	26.307	1.026	26.353	1.025	26.342
10	1.064	28.704	1.028	28.785	1.064	28.704	1.044	28.754	1.048	28.735	1.034	27.769	1.028	27.658	1.034	27.769	1.030	27.698	1.031	27.726
10-1L	1.047	25.937	1.024	26.029	1.047	25.937	1.033	25.992	1.037	25.982	1.044	24.986	1.025	24.908	1.044	24.986	1.033	24.936	1.036	24.955
10-2L	0.991	25.909	1.024	26.029	0.991	25.909	1.010	25.981	1.007	25.957	0.996	24.966	1.025	24.908	0.996	24.966	1.014	24.930	1.007	24.941
11	1.043	29.495	1.031	29.381	1.033	29.410	1.036	29.426	1.038	29.447	1.036	28.036	1.031	27.978	1.032	27.991	1.033	28.000	1.034	28.007
11L	-	-	-	-	-	-	-	-	-	-	0.983	24.526	1.027	24.555	0.983	24.526	1.009	24.545	1.004	24.539

Table 2. D-LSE of the substation-level current estimation results for Substation 7 (BHA) with circuit breaker c (CB c) current bad data. Magnitude ("M") is shown in pu, and the angle (∠) is in degrees (°).

| Current | Measurement | | True Value | | Substation Level | | | | NR |
| | | | | | Current Estimation | | | | |
	M (pu)	∠°	M (pu)	∠°	M (pu)	∠°	ERF_M	$ERF_∠$	
CB a	**0.273**	**76.108**	**0.277**	**75.412**	**0.274**	**76.955**	**1.37**	**0.45**	**11.43**
CB b	**0.019**	**87.367**	**0.001**	**−93.523**	**0.016**	**−56.099**	**1.18**	**4.83**	**20.95**
CB c	**0.287**	**74.055**	**0.277**	**−104.604**	**0.068**	**−98.092**	**0.05**	**27.44**	**32.38**
CB d	0.665	−95.414	0.683	−94.674	0.672	−94.559	1.69	6.43	2.99
CB e	0.045	83.710	0.000	−95.544	0.020	55.465	2.23	1.19	4.35
CB f	0.690	85.915	0.683	85.326	0.680	86.016	2.55	0.85	1.56
CB g	0.652	89.972	0.665	90.739	0.653	89.762	1.11	0.78	0.41
CB h	0.007	96.894	0.000	−94.520	0.005	85.032	1.33	1.07	0.31
CB i	0.675	−89.509	0.665	−89.262	0.672	−89.405	1.47	1.73	0.47
CB j	0.268	−91.236	0.253	−91.972	0.264	−90.679	1.33	0.57	0.69
CB k	0.243	88.654	0.253	88.030	0.247	88.361	1.71	1.89	0.69
TL127-1	**0.279**	**77.299**	**0.278**	**75.455**	**-**	**-**	**-**	**-**	**11.43**
TL127-2	**0.308**	**75.560**	**0.278**	**75.455**	**-**	**-**	**-**	**-**	**32.38**
TL78-1	0.682	−92.871	0.682	−94.675	-	-	-	-	2.99
TL78-2	0.683	−93.321	0.682	−94.675	-	-	-	-	1.56
TL67-1	0.648	89.479	0.665	90.738	-	-	-	-	0.41
TL67-2	0.662	90.639	0.665	90.738	-	-	-	-	0.47
TL77L	0.504	−90.705	0.505	−91.971	-	-	-	-	0.69
Average	**-**	**-**	**-**	**-**	**-**	**-**	**1.46**	**4.29**	**-**

Table 3. D-LSE of the substation-level current estimation results for Substation 7 (BHA) with circuit breaker c (CB c) current and injection current from TL67-2 bad data. Magnitude ("M") is shown in pu, and the angle (∠) is in degrees (°).

| Current | True Value | | Measurement | | Substation Level | | | | NR |
| | | | | | Current Estimation | | | | |
	M (pu)	∠°	M (pu)	∠°	M (pu)	∠°	ERF_M	$ERF_∠$	
CB a	**0.277**	**75.412**	**0.264**	**75.867**	**0.208**	**75.505**	**0.19**	**4.88**	**8.30**
CB b	**0.001**	**−93.523**	**0.014**	**−95.401**	**0.138**	**76.403**	**0.10**	**0.01**	**22.65**
CB c	**0.277**	**−104.604**	**0.274**	**77.099**	**0.067**	**−45.902**	**0.01**	**3.10**	**30.95**
CB d	0.683	−94.674	0.688	−95.953	0.685	−94.962	2.94	4.43	2.19
CB e	0.000	−95.544	0.015	84.897	0.013	−5.012	1.15	1.99	2.93
CB f	0.683	85.326	0.675	83.953	0.687	84.050	1.82	1.08	1.69
CB g	**0.665**	**90.739**	**0.666**	**89.695**	**0.845**	**89.758**	**0.01**	**1.06**	**26.70**
CB h	**0.000**	**−94.520**	**0.022**	**85.946**	**0.348**	**90.385**	**0.06**	**0.98**	**48.71**
CB i	**0.665**	**−89.262**	**0.684**	**−90.771**	**0.179**	**−94.176**	**0.04**	**0.31**	**75.41**
CB j	0.253	−91.972	0.261	−90.571	0.251	−91.487	6.14	2.89	1.62
CB k	0.253	88.030	0.269	89.445	0.259	88.558	2.47	2.68	1.62

Table 3. *Cont.*

Current	True Value		Measurement		Substation Level				NR
					Current Estimation		ERF$_M$	ERF$_\angle$	
	M (pu)	∠°	M (pu)	∠°	M (pu)	∠°			
TL127-1	**0.278**	**75.455**	**0.291**	**75.604**	**-**	**-**	**-**	**-**	**8.30**
TL127-2	**0.278**	**75.455**	**0.279**	**76.849**	**-**	**-**	**-**	**-**	**30.95**
TL78-1	0.682	−94.675	0.692	−92.515	-	-	-	-	2.19
TL78-2	0.682	−94.675	0.698	−95.079	-	-	-	-	1.69
TL67-1	**0.665**	**90.738**	**0.676**	**89.497**	**-**	**-**	**-**	**-**	**26.70**
TL67-2	**0.665**	**90.738**	**0.675**	**-88.369**	**-**	**-**	**-**	**-**	**75.41**
TL77L	0.505	−91.971	0.501	−91.942	-	-	-	-	1.62
Average	-	-	-	-	-	-	1.36	2.13	-

3.1.4. Steady State with Gaussian White Noise and Voltage Measurement Bad Data at Area Level

The substation level of the D-LSE identifies bad data through current estimation, which raises the substation bad data flag and informs the area level regarding the handing over process. The area level filters out the substation that detected bad data and conducts the LSE. Yet, there can be bad voltage phasor measurements at the area level, since substation level bad data detection is limited to the current measurements. Thus, bad data identification is conducted at the area level. The bad data considered were the reverse phasor of the voltage measurement in Substations 6 and 10. The results are presented in Table 4 for the area level and network level.

Table 4. Voltage estimation from the area level and network level for modified two-area four-machine power system model under a steady state with bad voltage data in Substations 6 and 10 (not detected by the substation level) included in area level. Magnitude ("M") is shown in pu, and the angle (∠) is in degrees (°).

Substation		Measurement		True Value		Area Level					Network Level			
						Voltage Estimation		ERF$_M$	ERF$_\angle$	NR	Voltage Estimation		ERF$_M$	ERF$_\angle$
ID	Type	M (pu)	∠°	M (pu)	∠°	M (pu)	∠°				M (pu)	∠°		
5	RBA	0.987	34.485	1.031	34.009	1.014	34.043	2.48	14.21	0.93	1.011	34.085	2.15	6.31
5L	SBA	1.021	28.265	1.027	30.588	1.023	29.625	1.60	2.41	1.61	1.022	29.319	1.12	1.83
6	**SBA**	**1.037**	**−144.806**	**1.030**	**34.761**	**1.036**	**−55.029**	**1.21**	**2.00**	**43.41**	**1.031**	**28.187**	**5.23**	**27.31**
6L	SBA	0.983	33.094	1.027	32.707	1.034	32.939	6.84	1.67	3.04	1.032	33.496	9.52	0.49
12	SBA	1.021	34.723	1.035	34.927	1.030	34.653	2.69	0.74	2.26	1.024	34.474	1.36	0.45
7	BHA	1.056	32.988	1.033	34.559	1.037	33.983	6.39	2.73	2.61	1.038	39.849	4.51	0.30
7L	SBA	1.007	34.388	1.032	33.992	1.023	34.068	2.85	5.18	1.33	1.015	34.084	1.45	4.30
8	DBDBA	1.026	32.697	1.042	31.550	1.035	31.935	2.38	2.98	0.93	1.037	31.849	3.09	3.83
13	SBA	1.042	30.516	1.033	29.046	1.031	29.419	4.25	3.94	3.14	1.039	29.295	1.52	5.91
9	SBA	1.011	28.623	1.032	28.662	1.022	28.824	2.03	0.24	2.23	1.015	28.692	1.23	1.31
9L	SBA	1.010	27.395	1.031	27.629	1.013	27.796	1.16	1.40	3.41	1.011	27.697	1.06	3.45
10	**SBA**	**1.040**	**−151.395**	**1.029**	**28.551**	**1.020**	**−61.421**	**1.31**	**2.00**	**38.40**	**1.024**	**17.935**	**2.34**	**16.95**
10-1L	SBA	1.036	24.548	1.025	25.810	1.018	25.127	1.49	1.85	1.61	1.033	25.238	1.34	2.21
10-2L	SBA	1.013	27.319	1.025	25.800	1.023	25.267	6.78	2.85	2.26	1.019	25.015	1.88	1.94
11	DBSBA	1.005	28.381	1.031	28.427	1.022	28.492	2.75	0.71	2.20	1.017	28.244	1.86	0.25
11L	MTBA	1.003	24.564	1.027	25.005	1.033	25.589	4.25	0.76	1.04	1.039	25.342	2.12	1.31
Average		-	-	-	-	-	-	3.15	2.85	-	-	-	2.61	4.88

3.2. IEEE 68 Bus Power System (System 2)

The IEEE 68 bus power system model simulation and D-LSE implementation were based on the system shown in Figure 12. The IEEE 68 bus system demonstrates the scalability of the D-LSE. The IEEE 68 bus power system model comprises five areas with 16 conventional synchronous generators [34]. Area 1 consists of generators G1 to G9. Area 2 consists of generators G10 to G13. Areas 3, 4, and 5 contain a single generator per area, namely G14, G15, and G16. The D-LSE's area level and network level were implemented on the IEEE 68 bus power system due to the limitations of implementing the substation arrangements of the simulation platform. This test system had no bus overlaps between areas, thus conveniently designating the area level with the buses in designated areas. Furthermore, the whole test system was considered a single entity at the network level.
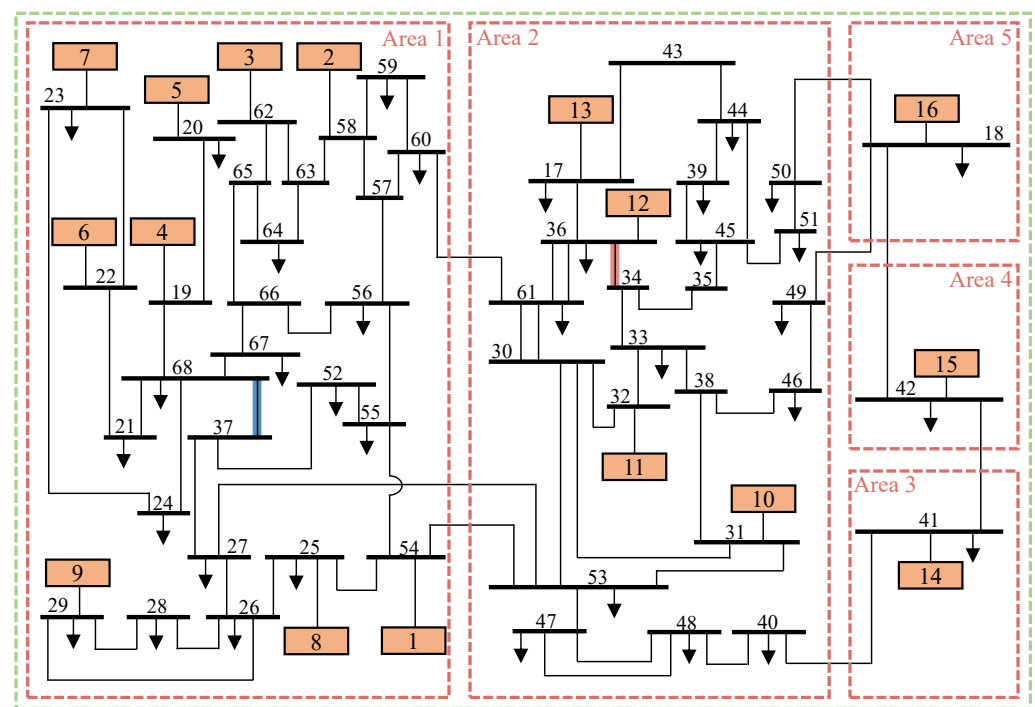
Figure 12. IEEE 68 bus benchmark system [34] indicating D-LSE area level and network level. Topology was changed from Topology S2A (fully connected network) to Topology S2B by removing TL68-37, which is indicated in blue. Topology was changed from Topology S2B to Topology S2C by removing TL36-34, which is shown in red.

The area level and network level were implemented into the IEEE 68 bus power system by considering all buses as SBAs, thus neglecting generator buses (Bus ID 1–16), since the generator buses were integrated into the generator module in the simulation model.

3.2.1. Steady State with Gaussian White Noise for Topology Change

The D-LSE was tested for the topology changes detected by H-TNTP-PMU [28] for the IEEE 68 bus system. The topology changes considered for the IEEE 68 bus system were Topology S2B and Topology S2C. The topologies were selected to avoid bus isolation, where pre- and postconditions are stable. Table A2 presents the steady state D-LSE voltage estimation for the area level and network level in Topology S2A. Table 5 presents the steady state voltage estimates for the D-LSE area level in Topology S2B and Topology S2C. In both topology changes, an alternative rerouting path was available. The topology was changed from Topology S2A (fully connected network) to Topology S2B by removing TL68-37 in Area 1, and the topology was changed from Topology S2B to Topology S2C subsequently by removing another single line in Area 2, TL36-34, as shown in Figure 12. The topology changes are shown in Figure 13.

Table 5. Voltage estimation from the area level for the IEEE 68 bus power system model under a steady state for Topology S2B (TL68-37 outage) and Topology S2C (TL36-34 outage). Magnitude ("M") is shown in pu, and the angle (∠) is in degrees (°).

Bus ID	Topology C						Topology D					
	Measurement		True Value		Voltage Estimation		Measurement		True Value		Voltage Estimation	
	M (pu)	∠°	M (pu)	∠°	M (pu)	∠°	M (pu)	∠°	M (pu)	∠°	M (pu)	∠°
17	0.994	−5.728	1.025	−5.734	1.011	−5.731	1.011	−5.786	1.020	−5.777	1.016	−5.780
18	1.022	42.489	0.993	42.569	1.006	42.539	0.964	51.605	0.992	51.672	0.979	51.645
19	1.059	31.660	1.049	31.811	1.053	31.746	1.044	35.166	1.048	35.251	1.047	35.213
20	0.986	30.285	0.990	30.379	0.989	30.341	0.997	33.825	0.990	33.818	0.993	33.821
21	1.053	29.737	1.030	29.849	1.040	29.808	1.015	33.192	1.030	33.289	1.024	33.246
22	1.019	34.607	1.049	34.543	1.038	34.569	1.091	38.136	1.049	37.987	1.065	38.049
23	1.011	34.164	1.044	34.254	1.030	34.219	1.013	37.788	1.043	37.698	1.032	37.732
24	1.047	27.512	1.036	27.378	1.040	27.432	1.004	30.743	1.035	30.814	1.023	30.788
25	1.023	18.245	1.062	18.333	1.048	18.294	1.091	22.383	1.060	22.408	1.073	22.398
26	1.038	16.311	1.061	16.344	1.052	16.330	1.034	20.336	1.059	20.370	1.049	20.355
27	1.100	14.276	1.052	14.245	1.071	14.258	1.046	18.212	1.048	18.246	1.047	18.234
28	1.006	19.393	1.055	19.465	1.034	19.435	1.087	23.492	1.053	23.498	1.066	23.495
29	1.011	22.201	1.053	22.095	1.037	22.143	1.012	26.150	1.052	26.131	1.037	26.138
30	1.027	11.322	1.051	11.321	1.041	11.321	1.042	15.762	1.036	15.818	1.038	15.798
31	1.106	13.817	1.056	13.880	1.077	13.855	1.090	19.293	1.044	19.347	1.064	19.326
32	1.056	15.262	1.048	15.259	1.052	15.260	0.997	24.060	1.043	24.143	1.024	24.111
33	1.089	11.441	1.052	11.424	1.067	11.431	1.094	21.758	1.049	21.747	1.069	21.752
34	1.112	5.616	1.059	5.598	1.079	5.605	1.024	19.394	1.050	19.425	1.041	19.413
35	1.041	5.544	1.007	5.529	1.021	5.534	0.982	18.287	0.996	18.350	0.991	18.324
36	1.063	1.642	1.036	1.645	1.048	1.644	1.001	1.171	1.028	1.173	1.018	1.172
37	1.071	14.313	1.049	14.358	1.057	14.340	1.058	18.274	1.045	18.300	1.050	18.288
38	1.013	13.570	1.054	13.555	1.036	13.561	1.012	20.413	1.043	20.340	1.032	20.372
39	1.025	−6.494	0.997	−6.481	1.009	−6.487	0.926	−1.013	0.970	−1.010	0.952	−1.011
40	1.018	20.482	1.070	20.558	1.048	20.529	1.085	28.267	1.051	28.243	1.065	28.253
41	1.048	49.142	1.000	49.226	1.021	49.191	0.986	56.902	0.999	56.642	0.994	56.737
42	1.009	43.177	0.999	43.279	1.004	43.236	1.031	51.515	0.999	51.537	1.012	51.528
43	0.979	−0.596	1.008	−0.597	0.997	−0.597	1.024	−2.577	0.987	−2.588	1.002	−2.584
44	0.992	−5.976	1.007	−5.980	1.000	−5.979	0.941	−2.447	0.986	−2.451	0.969	−2.450
45	1.047	5.340	1.089	5.344	1.071	5.342	0.943	15.546	0.990	15.510	0.972	15.523
46	0.981	14.338	1.032	14.390	1.012	14.372	0.980	21.564	1.020	21.470	1.003	21.511
47	1.112	12.917	1.074	12.912	1.088	12.914	1.070	17.943	1.057	17.920	1.063	17.929
48	1.083	14.805	1.077	14.754	1.080	14.773	1.042	19.887	1.060	19.980	1.052	19.942
49	1.040	17.435	1.012	17.492	1.024	17.469	1.034	24.890	0.999	24.924	1.012	24.912
50	1.024	22.865	1.004	22.801	1.011	22.827	0.988	32.684	0.998	32.543	0.995	32.601
51	1.052	9.546	1.013	9.527	1.028	9.535	0.989	19.624	0.999	19.568	0.995	19.589
52	1.060	14.362	1.045	14.422	1.051	14.395	1.023	18.383	1.042	18.335	1.035	18.355

Table 5. *Cont.*

Bus ID	Topology C						Topology D					
	Measurement		*True Value*		Voltage Estimation		*Measurement*		*True Value*		Voltage Estimation	
	M (pu)	**∠°**	**M (pu)**	**∠°**	**M (pu)**	**∠°**	**M (pu)**	**∠°**	**M (pu)**	**∠°**	**M (pu)**	**∠°**
53	1.028	12.202	1.058	12.263	1.046	12.237	1.054	17.025	1.044	17.029	1.048	17.027
54	1.103	17.226	1.056	17.207	1.072	17.215	1.049	21.363	1.053	21.323	1.051	21.338
55	1.003	15.623	1.043	15.623	1.028	15.623	1.022	19.493	1.040	19.496	1.032	19.495
56	1.053	18.954	1.022	18.969	1.033	18.963	1.036	22.407	1.018	22.447	1.026	22.432
57	0.998	19.470	1.019	19.562	1.011	19.529	0.977	22.954	1.014	22.856	1.001	22.900
58	0.995	20.236	1.020	20.270	1.010	20.256	1.028	23.643	1.015	23.559	1.020	23.589
59	0.996	17.665	1.012	17.720	1.006	17.696	1.013	20.862	1.005	20.908	1.008	20.891
60	1.049	16.996	1.012	17.025	1.027	17.013	0.999	20.212	1.005	20.166	1.002	20.183
61	1.059	7.635	1.034	7.631	1.045	7.633	1.044	9.844	1.018	9.851	1.027	9.848
62	1.071	23.428	1.026	23.347	1.045	23.378	0.985	26.585	1.023	26.714	1.009	26.662
63	1.056	22.239	1.022	22.309	1.037	22.284	1.051	25.657	1.019	25.651	1.032	25.654
64	1.036	22.392	1.064	22.483	1.053	22.445	1.104	25.719	1.060	25.846	1.077	25.794
65	0.980	22.959	1.023	22.876	1.004	22.912	1.033	26.261	1.020	26.280	1.025	26.272
66	1.018	21.944	1.022	21.838	1.020	21.876	0.997	25.174	1.019	25.267	1.010	25.229
67	1.045	24.576	1.016	24.482	1.029	24.516	0.994	27.985	1.015	27.915	1.006	27.944
68	0.987	27.076	1.030	27.204	1.013	27.153	0.998	30.683	1.029	30.641	1.017	30.658
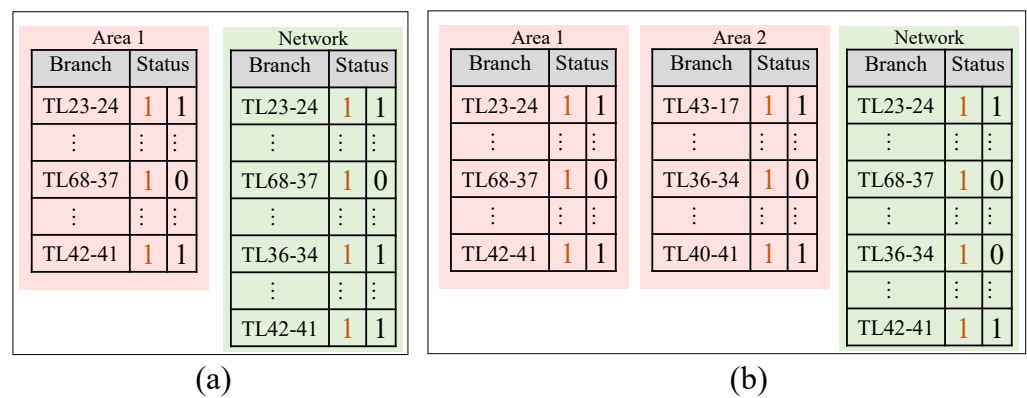
Figure 13. The topology change detected by H-TNTP-PMU Level 2-Area and H-TNTP Level 3 [28]. (**a**) Topology S2A (fully connected) to Topology S2B. (**b**) Topology S2B to Topology S2C.

3.3. Discussion

The computational efficiency was compared considering the analysis conducted in Table 6. The D-LSEs were evaluated for practical computational overhead with 50 trials on an Intel Xeon(R) Gold 3.3 GHz system with 63.7 GB RAM for all test cases present in Tables A1 and A2. The execution time was calculated using (12). j is either the substation level, area level, or network level. It is important to note that this analysis did not account for communication latency or other processing delays. The computational time within the PMU data rate window as a percentage is shown in the last column of Table 6.

$$LSE\ Time(T_{LSE\_j}) = T_{MF} + T_{MS}\ ;\ where\ T_{MS} = T_{MS}\ or\ (T_{MS1} + T_{MS2}) \tag{12}$$
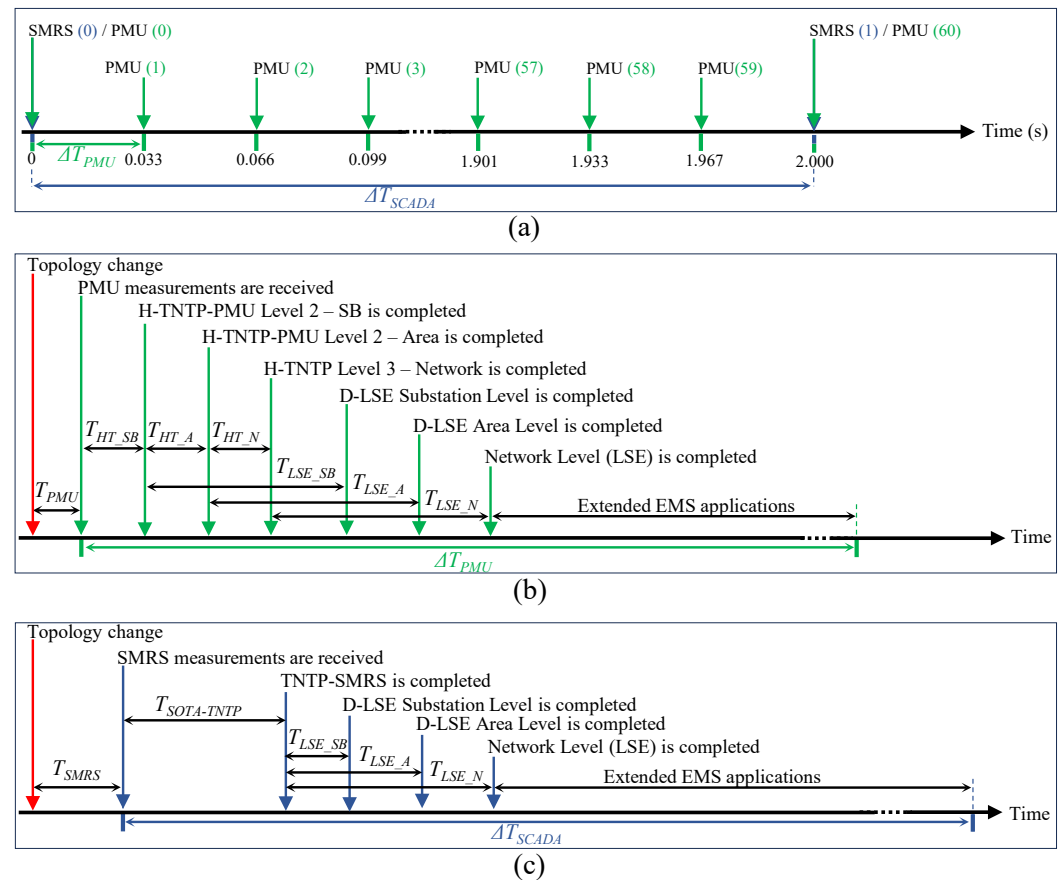
Table 6. Computational time estimated for the substation level, area level, and network level for modified two-area four-machine power system model under steady state.

System	Level		Matrix Forming (μs) (T_{MF})	LSE Matrix Solving (μs) (T_{MS})	*LSE Time* (μs)	Percentage from PMU Data Rate (%)
System A	Substation	SBA	0.3536 ± 0.0362	0.9834 ± 0.0216	1.3370 ± 0.0537	0.004
		RBA	0.2342 ± 0.0401	0.7336 ± 0.0273	0.9678 ± 0.0539	0.003
		DBSBA	0.6780 ± 0.0415	1.3920 ± 0.0794	2.0700 ± 0.0925	0.006
		DBDBA	0.8320 ± 0.0769	1.9922 ± 0.1020	2.8242 ± 0.1304	0.009
		BHA	1.1480 ± 0.0971	2.3200 ± 0.1097	3.4680 ± 0.1344	0.010
	Area	Area 1	3.4281 ± 0.4797	64.4102 ± 2.9906	67.8383 ± 3.0216	0.204
		Area 1–2	0.8020 ± 0.0170	10.4201 ± 0.7057	11.2221 ± 0.8267	0.034
		Area 2	2.7210 ± 0.0378	80.6010 ± 3.3116	83.3220 ± 3.5157	0.250
	Network	-	4.9080 ± 0.1621	136.9012 ± 1.5680	141.8092 ± 1.6198	0.425
System B	Area	Area 1	22.6467 ± 0.4752	711.3356 ± 18.8965	724.2492 ± 19.5782	2.173
		Area 2	16.2833 ± 0.4528	415.6667 ± 13.3265	427.9500 ± 15.3395	1.284
		Area 3	0.6417 ± 0.0289	8.6026 ± 0.5887	9.2417 ± 0.7887	0.028
		Area 4	0.6213 ± 0.0197	8.4015 ± 0.3489	9.0228 ± 0.4139	0.027
		Area 5	0.6669 ± 0.0273	8.4153 ± 0.3287	9.0822 ± 0.4358	0.027
	Network	-	68.6017 ± 0.9396	2552.0658 ± 41.1131	2620.7017 ± 45.8850	7.863

As a system, the modified two-area four-machine power system is small, and the computation time was less compared to the IEEE 68 bus system. Furthermore, the substation-level and the area-level computational times demonstrate the value of the distributed architecture. Since these two levels can be processed in parallel, the overall computational time can be minimized compared to the network level. This is important for new applications requiring PMU-based state estimation, where the smaller computation overhead is taken by TNTP [28] and LSE. Thus, it allows for higher computational flexibility for the new applications.

H-TNTP-PMU updates the network model in every PMU measurement frame, and SOTA-TNTP updates the network model in every SCADA measurement frame. The PMU and SMRS sampling at 30 Hz (every 33.33 ms) and every 2 s, respectively, is presented in a timeline as shown in Figure 14a. Due to the uncertainty of the instance, the network topology change occurred with respect to the PMU and SCADA samples collected; two possible scenarios in the topology identification-based flow can be defined as discussed in [28]. An extension to the same timeline interpretation, including three levels, is shown in Figure 14b,c. The delay between the instance the topology change occurred, and the next sample collected by the PMU and SCADA are defined as T_{PMU} and T_{SMRS}, respectively. $T_{SOTA-TNTP}$ is the time taken to complete SOTA TNTP, while T_{HT_k} refers to the H-TNTP-PMU completion time, where k refers to either the substation level (SB), area level (A), or network level (N). T_{LSE_s} refers to the time it takes to complete LSE in each level, where s is either the substation level (SB), area level (A), or network level (N). The time analysis shown in Table 7 was conducted for 50 trials for the Topology S1A to Topology S1B change discussed in Section 3.1.1. It is important to state that out of the 50 trials, 14% of the time the T_{SMRS} was less than 33.33 ms.

Figure 14. (**a**) The PMU and SMRS sampling timeline. (**b**) The timeline for estimation utilizing H-TNTP-PMU as the topology processor. (**c**) The timeline for estimation utilizing SOTA TNTP as the topology processor.

Table 7. Computational time estimated for D-LSE at the substation level, area level, and network level for modified two-area four-machine power system model under steady state.

Time Compoment	Level	Topology Processor	
		H-TNTP-PMU	**SOTA TNTP**
Sampling Delay (s)	-	0.017 ± 0.009	1.062 ± 0.588
Topology (µs)	Substation	7.122 ± 0.828	-
	Area	9.514 ± 0.783	-
	Network	11.365 ± 0.658	1.054 ± 0.0274
LSE (µs)	Substation	2.172 ± 0.164	
	Area	82.776 ± 3.857	
	Network	141.781 ± 2.428	

A summarized comparison of the three levels of the D-LSE is presented in Table 8. It can be seen that the substation level's highest computational time was less than that of the area level. Furthermore, the area level's highest computational time was less than the network level's. The robustness considers the ability to accurately estimate under noise (low: $ERF < 2$, medium: $2 < ERF < 3$, and high: $3 < ERF$), which is analyzed using the ERF in Tables A1 and A2. The resiliency considers estimation algorithm accuracy (low: $ERF > 4$ and medium: $ERF \leq 4$) under bad data in measurements, which are analyzed using the ERF in Sections 3.1.2–3.1.4.

Table 8. Comparison of proposed D-LSE levels.

Factor	Level		
	Substation	**Area**	**Network**
Computational Efficiency	Low	Medium	High
Robustness	High	Medium	Medium
Resiliency	Low	Medium	Medium

4. Conclusions

Modern power system operation is becoming complex and dynamic. Linear state estimation is a promising solution for state estimation with synchrophasor measurements. However, LSE is computationally inefficient for large power systems, and the state-of-the-art transmission network topology processing limits the true potential of LSE. An efficient, resilient, and robust multilevel distributed linear state estimation based on a hierarchical transmission network topology processing that updates the network model at the PMU rate has been presented in this paper. Using an efficient and reliable H-TNTP with synchrophasor data enables the practical implementation of a multilevel D-LSE for power systems of any scale. The typical results obtained with the multilevel D-LSE implemented on the modified IEEE two-area four-machine system model and the IEEE 68 bus system model demonstrate improved computational efficiency, resiliency against bad data, and robustness against noisy measurements. In addition, LSE at the network level integrated with the H-TNTP-PMU provides redundancy to the substation-level and area-level D-LSE. Future work includes investigating and developing security assessments for bulk power systems based on H-TNTP, multilevel D-LSE, and synchrophasor measurements with optimal usage.

Abbreviations

The following abbreviations are used in this manuscript:

BBM	Bus branch mode
BHA	Breaker and half arrangement
CCN	Cellular computational network
DBDBA	Double bus double breaker arrangement

DBSBA	Double bus single breaker arrangement
D-LSE	Distributed linear state estimation
ERF	Error reduction factor
GWN	Gaussian white noise
H-TNTP	Hierarchical transmission network topology processing
H-TNTP-PMU	Synchrophasor-based hierarchical transmission network topology processing
KCL	Kirchhoff's Current Law
LSE	Linear state estimation
MTBA	Main and transfer bus arrangement
NCM	Node connectivity matrix
PMU	Phasor measurement unit
RBA	Ring bus arrangement
RTDS	Real-Time Digital Simulator
SBA	Single bus arrangement
SCADA	Supervisory control and data acquisition
SMRS	Supervisory control and data acquisition system monitoring of relay signals
SOTA	State of the art
TNTP	Transmission network topology processing
TNTP-SMRS	Supervisory control and data acquisition system monitoring of relay signal-based transmission network topology processing
TVE	Total error vector

Appendix A. Fully Connected Topology Voltage Estimation

Table A1. Voltage estimation at the substation level, area level, and network level for modified two-area four-machine power system model (Topology S1A) under a steady state and the error reduction factor (*ERF*) analysis. Magnitude ("M") is shown in pu, and the angle ($\angle$) is in degrees (°).

Substation		Measurement		True Value		Substation Level				Area Level				Network Level			
						Voltage Estimation				Voltage Estimation				Voltage Estimation			
ID	Type	M (pu)	$\angle$°	M (pu)	$\angle$°	M (pu)	$\angle$°	ERF_M	$ERF_\angle$	M (pu)	$\angle$°	ERF_M	$ERF_\angle$	M (pu)	$\angle$°	ERF_M	$ERF_\angle$
5	RBA	1.000	33.908	1.031	34.009	1.027	33.990	8.30	5.19	1.018	33.964	2.34	2.24	1.014	33.952	1.83	1.75
5L	SBA	1.041	30.715	1.027	30.588	1.041	30.715	-	-	1.033	30.635	2.50	2.67	1.036	30.653	1.63	1.95
6	SBA	1.074	34.620	1.030	34.761	1.074	34.620	-	-	1.046	34.711	2.73	2.81	1.052	34.687	1.99	1.90
6L	SBA	0.992	32.673	1.027	32.707	0.992	32.673	-	-	1.012	32.693	2.38	2.40	1.006	32.686	1.62	1.58
12	SBA	1.020	34.793	1.035	34.927	1.020	34.793	-	-	1.028	34.877	2.23	2.71	1.027	34.849	1.90	1.73
7	BHA	1.063	34.692	1.033	34.559	1.039	34.573	5.73	9.78	1.044	34.613	2.82	2.47	1.052	34.633	1.62	1.80
7L	SBA	1.012	33.933	1.032	33.992	1.012	33.933	-	-	1.023	33.966	2.28	2.32	1.020	33.961	1.69	1.93
8	DBDBA	1.043	31.449	1.042	31.550	1.042	31.532	7.80	5.75	1.043	31.511	2.46	2.61	1.043	31.487	2.00	1.61
13	SBA	1.030	29.066	1.033	29.046	1.030	29.066	-	-	1.032	29.055	2.29	2.33	1.032	29.059	1.88	1.56
9	SBA	1.016	28.611	1.032	28.662	1.016	28.611	-	-	1.026	28.644	2.84	2.86	1.022	28.632	1.56	1.72
9L	SBA	0.999	27.765	1.031	27.629	0.999	27.765	-	-	1.019	27.683	2.68	2.52	1.015	27.697	1.94	1.99
10	SBA	0.983	28.658	1.029	28.551	0.983	28.658	-	-	1.010	28.596	2.40	2.37	1.005	28.618	1.89	1.60
10-1L	SBA	1.015	25.902	1.025	25.810	1.015	25.902	-	-	1.021	25.848	2.81	2.46	1.020	25.866	1.93	1.64
10-2L	SBA	1.029	25.861	1.025	25.800	1.029	25.861	-	-	1.027	25.823	2.30	2.61	1.027	25.836	1.75	1.68
11	DBSBA	0.982	28.470	1.031	28.427	1.022	28.437	5.41	4.05	1.011	28.444	2.49	2.56	1.005	28.451	1.86	1.76
11L	MTBA	1.029	25.033	1.027	25.005	1.029	25.033	-	-	1.028	25.016	2.42	2.53	1.028	25.020	1.88	1.92
Average		-	-	-	-	-	-	6.81	6.19	-	-	2.50	2.53	-	-	1.81	1.76

Table A2. Voltage estimation at the area level and network level for IEEE 68 bus power system model (Topology S2A) under a steady state and the error reduction factor (*ERF*) analysis. Magnitude ("M") is shown in pu, and the angle (∠) is in degrees (°).

Bus ID	Measurement		True Value		Area Level				Network Level			
					Voltage Estimation		ERF_M	$ERF_\angle$	Voltage Estimation		ERF_M	$ERF_\angle$
	M (pu)	∠°	M (pu)	∠°	M (pu)	∠°			M (pu)	∠°		
17	1.044	−5.747	1.025	−5.728	1.033	−5.736	2.38	2.40	1.037	−5.738	1.59	1.93
18	0.992	42.644	0.993	42.752	0.993	42.705	2.77	2.31	0.993	42.683	1.84	1.56
19	1.021	24.180	1.052	24.099	1.040	24.133	2.73	2.34	1.032	24.145	1.54	1.76
20	0.978	22.578	0.992	22.673	0.986	22.639	2.43	2.76	0.985	22.614	1.91	1.61
21	1.072	22.065	1.036	22.135	1.051	22.109	2.36	2.70	1.056	22.100	1.75	1.99
22	1.072	26.733	1.052	26.797	1.059	26.770	2.57	2.33	1.064	26.758	1.59	1.65
23	1.058	26.411	1.047	26.510	1.051	26.470	2.67	2.47	1.054	26.449	1.68	1.60
24	1.034	19.771	1.044	19.691	1.040	19.719	2.44	2.85	1.038	19.734	1.93	1.87
25	1.099	20.103	1.063	20.038	1.077	20.067	2.60	2.24	1.086	20.073	1.59	1.83
26	1.095	19.052	1.060	19.011	1.074	19.028	2.61	2.36	1.078	19.035	1.95	1.67
27	1.060	17.402	1.048	17.349	1.053	17.369	2.35	2.66	1.054	17.377	1.90	1.87
28	1.082	22.071	1.054	22.136	1.065	22.110	2.52	2.50	1.071	22.096	1.61	1.64
29	1.083	24.779	1.052	24.767	1.065	24.772	2.46	2.60	1.071	24.774	1.68	1.81
30	1.018	11.592	1.051	11.535	1.037	11.560	2.47	2.30	1.030	11.568	1.56	1.70
31	1.054	14.147	1.055	14.170	1.055	14.161	2.73	2.65	1.055	14.158	1.87	2.00
32	1.047	15.483	1.048	15.417	1.048	15.440	2.32	2.81	1.048	15.459	1.81	1.56
33	1.063	11.612	1.051	11.561	1.056	11.581	2.39	2.56	1.058	11.589	1.62	1.87
34	1.109	5.660	1.059	5.664	1.078	5.663	2.68	2.31	1.088	5.662	1.72	1.77
35	1.025	5.583	1.007	5.598	1.015	5.591	2.34	2.34	1.017	5.589	1.91	1.60
36	1.002	1.652	1.036	1.654	1.024	1.653	2.69	2.35	1.016	1.653	1.68	1.76
37	1.031	18.141	1.043	18.139	1.039	18.140	2.64	2.76	1.036	18.141	1.66	1.59
38	1.070	13.748	1.053	13.803	1.059	13.778	2.71	2.22	1.064	13.770	1.61	1.68
39	1.004	−6.462	0.997	−6.440	1.000	−6.449	2.25	2.29	1.000	−6.454	1.99	1.62
40	1.114	20.919	1.070	20.920	1.089	20.920	2.27	2.31	1.098	20.920	1.58	1.60
41	1.013	49.487	1.000	49.514	1.005	49.502	2.62	2.26	1.008	49.499	1.60	1.78
42	1.034	43.548	0.999	43.515	1.012	43.527	2.69	2.62	1.017	43.535	1.95	1.62
43	0.957	−5.967	1.007	−5.945	0.985	−5.954	2.30	2.41	0.978	−5.958	1.74	1.63
44	0.992	−5.952	1.007	−5.951	1.000	−5.952	2.27	2.78	0.999	−5.952	1.79	1.75
45	0.971	5.434	1.009	5.419	0.994	5.425	2.47	2.37	0.987	5.428	1.69	1.67
46	1.040	14.695	1.031	14.628	1.035	14.654	2.41	2.64	1.036	14.662	1.93	1.98
47	1.070	13.256	1.073	13.297	1.072	13.283	2.51	2.79	1.072	13.277	1.76	1.98
48	1.052	15.070	1.077	15.131	1.068	15.104	2.58	2.27	1.064	15.093	1.91	1.63
49	1.021	17.771	1.012	17.720	1.016	17.738	2.39	2.77	1.017	17.746	1.73	1.99
50	1.054	23.026	1.004	22.934	1.024	22.973	2.58	2.38	1.036	22.983	1.58	1.87
51	1.045	9.623	1.012	9.619	1.026	9.620	2.43	2.62	1.031	9.621	1.79	1.83
52	1.044	17.203	1.041	17.261	1.042	17.238	2.60	2.51	1.043	17.231	1.63	1.93

Table A2. *Cont.*

Bus ID	Measurement		True Value		Area-Level				Network Level			
					Voltage Estimation		ERF_M	$ERF_\angle$	Voltage Estimation		ERF_M	$ERF_\angle$
	M (pu)	**∠°**	**M (pu)**	**∠°**	**M (pu)**	**∠°**			**M (pu)**	**∠°**		
53	1.106	12.611	1.057	12.661	1.078	12.643	2.37	2.84	1.086	12.631	1.68	1.65
54	1.021	18.602	1.054	18.605	1.040	18.604	2.37	2.31	1.035	18.603	1.69	1.69
55	0.994	16.894	1.042	16.939	1.023	16.919	2.47	2.28	1.014	16.914	1.72	1.80
56	0.999	17.625	1.026	17.686	1.014	17.662	2.24	2.52	1.012	17.649	1.93	1.67
57	1.059	18.134	1.023	18.110	1.038	18.120	2.37	2.35	1.046	18.123	1.58	1.86
58	1.039	18.760	1.024	18.739	1.031	18.747	2.23	2.56	1.033	18.751	1.79	1.81
59	1.038	16.439	1.016	16.372	1.026	16.400	2.29	2.37	1.030	16.412	1.58	1.67
60	0.994	15.807	1.017	15.764	1.007	15.780	2.34	2.62	1.003	15.788	1.61	1.81
61	1.077	7.573	1.035	7.595	1.050	7.586	2.84	2.31	1.061	7.584	1.59	1.97
62	0.988	21.344	1.030	21.241	1.011	21.277	2.24	2.81	1.007	21.295	1.82	1.90
63	0.999	20.428	1.027	20.388	1.015	20.402	2.35	2.82	1.010	20.410	1.64	1.80
64	1.043	20.386	1.069	20.382	1.060	20.384	2.80	2.59	1.054	20.385	1.79	1.76
65	1.036	20.567	1.028	20.593	1.031	20.583	2.85	2.43	1.032	20.577	1.89	1.59
66	1.071	19.183	1.028	19.100	1.043	19.136	2.79	2.32	1.054	19.146	1.65	1.80
67	0.997	18.353	1.025	18.302	1.015	18.322	2.82	2.58	1.009	18.330	1.73	1.82
68	1.037	19.510	1.039	19.518	1.039	19.514	2.56	2.30	1.038	19.514	1.65	2.00
Average	-	-	-	-	-	-	2.50	2.52	-	-	1.73	1.77

References

1. Schweppe, F.C.; Wildes, J. Power System Static-State Estimation, Part I: Exact Model. *IEEE Trans. Power Appar. Syst.* **1970**, *PAS-89*, 120–125. [CrossRef]
2. Schweppe, F.C.; Rom, D.B. Power System Static-State Estimation, Part II: Approximate Model. *IEEE Trans. Power Appar. Syst.* **1970**, *PAS-89*, 125–130. [CrossRef]
3. Schweppe, F.C. Power System Static-State Estimation, Part III: Implementation. *IEEE Trans. Power Appar. Syst.* **1970**, *PAS-89*, 130–135. [CrossRef]
4. Cooper, A.; Bretas, A.; Meyn, S. Anomaly Detection in Power System State Estimation: Review and New Directions. *Energies* **2023**, *16*, 6678. [CrossRef]
5. Zhang, G.; Gao, W.; Li, Y.; Guo, X.; Hu, P.; Zhu, J. Detection of False Data Injection Attacks in a Smart Grid Based on WLS and an Adaptive Interpolation Extended Kalman Filter. *Energies* **2023**, *16*, 7203. [CrossRef]
6. PES-TR118. *State Estimation for Integrated Energy Systems: Motivations, Advances, and Challenges*; Technical Report; IEEE PES Energy Internet Coordinating Committee IEEE PES Working Group on Power System Static and Dynamic State Estimation: Blacksburg, VA, USA, 2023.
7. Liang, J.; Venayagamoorthy, G.K.; Harley, R.G. Wide-Area Measurement Based Dynamic Stochastic Optimal Power Flow Control for Smart Grids With High Variability and Uncertainty. *IEEE Trans. Smart Grid* **2012**, *3*, 59–69. [CrossRef]
8. Kar, S.; Hug, G.; Mohammadi, J.; Moura, J.M.F. Distributed State Estimation and Energy Management in Smart Grids: A Consensus + Innovations Approach. *IEEE J. Sel. Top. Signal Process.* **2014**, *8*, 1022–1038. [CrossRef]
9. Li, X.; Balasubramanian, P.; Sahraei-Ardakani, M.; Abdi-Khorsand, M.; Hedman, K.W.; Podmore, R. Real-Time Contingency Analysis With Corrective Transmission Switching. *IEEE Trans. Power Syst.* **2017**, *32*, 2604–2617. [CrossRef]
10. Abur, A.; Exposito, A.G. *Power System State Estimation: Theory and Implementation*; CRC Press: Boca Raton, FL, USA, 2004; Volume 24. [CrossRef]
11. Jones, K.D. Synchrophasor-Only Dynamic State Estimation & Data Conditioning. Ph.D. Thesis, Virginia Polytechnic Institute and State University, Blacksburg, VA, USA, 2013.
12. Phadke, A.; Thorp, J. *Synchronized Phasor Measurements and Their Applications*, 1st ed.; Springer: New York, NY, USA, 2008.
13. Farrokhabadi, M.; Vanfretti, L. State-of-the-art of topology processors for EMS and PMU applications and their limitations. In Proceedings of the IECON 2012—38th Annual Conference on IEEE Industrial Electronics Society, Montreal, QC, Canada, 25–28 October 2012; pp. 1422–1427. [CrossRef]

14. Cao, J.; Wan, Y.; Hua, H.; Yang, G. Performance modeling for data monitoring services in smart grid: A network calculus based approach. *CSEE J. Power Energy Syst.* **2020**, *6*, 610–618. [CrossRef]

15. Kong, X.; Chen, Y.; Xu, T.; Wang, C.; Yong, C.; Li, P.; Yu, L. A Hybrid State Estimator Based on SCADA and PMU Measurements for Medium Voltage Distribution System. *Appl. Sci.* **2018**, *8*, 1527. [CrossRef]

16. Zhao, J.; Gómez-Expósito, A.; Netto, M.; Mili, L.; Abur, A.; Terzija, V.; Kamwa, I.; Pal, B.; Singh, A.K.; Qi, J.; et al. Power System Dynamic State Estimation: Motivations, Definitions, Methodologies, and Future Work. *IEEE Trans. Power Syst.* **2019**, *34*, 3188–3198. [CrossRef]

17. Zhao, J.; Mili, L.; La Scala, M. A robust hybrid power system state estimator with unknown measurement noise. In *Advances in Electric Power and Energy*; John Wiley & Sons, Ltd.: Hoboken, NJ, USA, 2020; Chapter 8, pp. 231–253. [CrossRef]

18. Xie, L.; Choi, D.H.; Kar, S.; Poor, H.V. Fully Distributed State Estimation for Wide-Area Monitoring Systems. *IEEE Trans. Smart Grid* **2012**, *3*, 1154–1169. [CrossRef]

19. Kekatos, V.; Giannakis, G.B. Distributed Robust Power System State Estimation. *IEEE Trans. Power Syst.* **2013**, *28*, 1617–1626. [CrossRef]

20. Korres, G.N. A Distributed Multiarea State Estimation. *IEEE Trans. Power Syst.* **2011**, *26*, 73–84. [CrossRef]

21. Zhu, H.; Giannakis, G.B. Power System Nonlinear State Estimation Using Distributed Semidefinite Programming. *IEEE J. Sel. Top. Signal Process.* **2014**, *8*, 1039–1050. [CrossRef]

22. Guo, Y.; Wu, W.; Zhang, B.; Sun, H. A distributed state estimation method for power systems incorporating linear and nonlinear models. *Int. J. Electr. Power Energy Syst.* **2015**, *64*, 608–616. [CrossRef]

23. Jones, K.D.; Thorp, J.S.; Gardner, R.M. Three-phase linear state estimation using Phasor Measurements. In Proceedings of the 2013 IEEE Power Energy Society General Meeting, Vancouver, BC, Canada, 21–25 July 2013; pp. 1–5. [CrossRef]

24. Vanfretti, L.; Chow, J.H.; Sarawgi, S.; Fardanesh, B. A Phasor-Data-Based State Estimator Incorporating Phase Bias Correction. *IEEE Trans. Power Syst.* **2011**, *26*, 111–119. [CrossRef]

25. Yang, T.; Sun, H.; Bose, A. Two-level PMU-based linear state estimator. In Proceedings of the 2009 IEEE/PES Power Systems Conference and Exposition, Washington, DC, USA, 15–18 March 2009; pp. 1–6. [CrossRef]

26. Yang, T.; Sun, H.; Bose, A. Transition to a Two-Level Linear State Estimator—Part I: Architecture. *IEEE Trans. Power Syst.* **2011**, *26*, 46–53. [CrossRef]

27. Yang, T.; Sun, H.; Bose, A. Transition to a Two-Level Linear State Estimator—Part II: Algorithm. *IEEE Trans. Power Syst.* **2011**, *26*, 54–62. [CrossRef]

28. Madurasinghe, D.; Venayagamoorthy, G.K. An Efficient and Reliable Electric Power Transmission Network Topology Processing. *IEEE Access* **2023**, *11*, 127956–127973. [CrossRef]

29. Biswal, C.; Sahu, B.K.; Mishra, M.; Rout, P.K. Real-Time Grid Monitoring and Protection: A Comprehensive Survey on the Advantages of Phasor Measurement Units. *Energies* **2023**, *16*, 4054. [CrossRef]

30. Wu, L.; Venayagamoorthy, G.K.; Gao, J. Online Steady-State Security Awareness Using Cellular Computation Networks and Fuzzy Techniques. *Energies* **2021**, *14*, 148. [CrossRef]

31. McDonald, J.D. *Electric Power Substations Engineering*, 3rd ed.; CRC Press: Boca Raton, FL, USA, 2012.

32. Zhang, X.; Lu, C.; Lin, J.; Wang, Y. Experimental test of PMU measurement errors and the impact on load model parameter identification. *IET Gener. Transm. Distrib.* **2020**, *14*, 4593–4604. [CrossRef]

33. RTDS Technologies Inc. Real-Time Digital Power System Simulation. Available online: https://www.rtds.com (accessed on 15 April 2024).

34. Bikash Pal, B.C. *Robust Control in Power Systems*; Springer: New York, NY, USA, 2005.